DOCTORAL THESIS

Water-lubricated high-performance polymers

Prashant Gangwani

Machine Elements

LULEÅ
UNIVERSITY
OF TECHNOLOGY

Water-lubricated high-performance polymers

Prashant Gangwani

Supervisors:

Prof. Nazanin Emami

Division of Machine Elements
Department of Engineering Science and Mathematics
Luleå University of Technology, Sweden

Prof. Mitjan Kalin

Faculty of Mechanical Engineering
University of Ljubljana

UNIVERZA V LJUBLJANI
University of Ljubljana

ISSN: 1402-1544
ISBN: 978-91-8048-933-1 (print)
ISBN: 978-91-8048-934-8 (electronic)

Luleå, 2025

ACKNOWLEDGEMENTS

This thesis is the result of years of unwavering dedication, countless late nights, and moments of both doubt and triumph. From the very first spark of curiosity that led me down this path, I have faced challenges that tested my resolve and pushed me to grow beyond my perceived limits. There were days when progress seemed elusive and the mountain of work insurmountable, yet each setback became a stepping stone, strengthening my determination. It was in those moments of adversity that I discovered the power of resilience, finding within myself the courage to get back up again and continue the journey. Today, as I present the results of this extensive research, I am filled with profound gratitude for the perseverance that carried me through. This work is more than a collection of experiments and analysis, it is a testament to the transformative journey of learning, persistence, and the unwavering belief that every challenge can be overcome with dedication and passion.

Many thanks are due, first and foremost, to my Parents to whom I am indebted for their unwavering understanding and boundless support throughout this journey. They accepted my countless absences, recognizing the importance of my work. Their steadfast faith in my dreams has given me the freedom to pursue my goals without reservation, reminding me that love and encouragement are the greatest catalysts for success.

A special debt of gratitude is owed to my mentors, Professor Mitjan Kalin and Professor Nazanin Emami; without their guidance, I would never have reached the finish line. Their expertise and belief in me helped me navigate complex challenges, and the lessons I have learned from them will continue to guide me long after this thesis is complete.

When I began, I knew little about polymer composites. My colleagues, through thought-provoking discussions and by sharing their insights, greatly assisted me in acquiring the requisite knowledge and confidence to advance my research.

Equally, I am grateful to my friends, whose constant companionship and uplifting spirits lightened the feeling of being away from home for so long. All their reassuring words and shared moments of laughter reaffirmed that no matter the distance, I never was or will be alone in this venture.

To everyone who has been part of this adventure—whether through a word of encouragement, a moment of understanding, or a shared glass of Coca-Cola—I extend my heartfelt thanks. Your belief fuelled my passion and propelled me forward, transforming obstacles into opportunities and dreams into reality. This thesis stands as much yours as it is mine.

Prashant Gangwani
Luleå, December 2025

ABSTRACT

Polymer-composites are indispensable tribo-materials in a wide range of engineering applications, including gears, bearings, joint implants, and automotive components. In many of these applications the presence of liquid lubricant is unavoidable, requiring a thorough understanding of composite behaviour under lubricated conditions. However, with growing emphasis on environmental safety, the use of petroleum oil-based lubricants, especially near aqueous environments, such as ships, pumps and turbines, has become increasingly dubious. Estimates suggest that of the 30–40 million tonnes of lubricant used annually, around 55% may eventually re-enter the environment, with approximately 95% of these being petroleum-based. These systems contribute to emissions and resource depletion, driving interest in the development of lubricant technologies free from petroleum-derived products. Some potential replacements to them are acceptable alternate lubricants like esters and glycerol, or mere water, which is abundantly available and emission free. The tribological performance of polymer composites often differs between dry and lubricated conditions, as contribution from polymer and fillers are observed to vary across environments. While numerous studies have explored the role of various fillers in water lubricated conditions, limited knowledge is available on other alternate lubricants. More recently, the focus on polymer-composite side has shifted towards multi-filler systems, which, when working synergistically, can provide superior performance compared to having a single filler. However, the existing literature lacks clarity on several key aspects: including the individual roles of filler material and scale; the nature and effect of filler–filler and filler–lubricant interactions to overall performance. This thesis investigates these gaps and provides deeper insights into the mechanisms governing the lubricated tribological behaviour of multi-filler polymer composites.

Keywords:
Composites, Tribology, Fillers, Water lubrication, Acceptable alternate lubricants

APPENDED PAPERS

Paper A Prashant Gangwani, Mitjan Kalin, Nazanin Emami (2023)
Does a Compatibilizer Enhance the Properties of Carbon Fiber-Reinforced Composites?
Polymers (mdpi), DOI: 10.3390/polym15234608
Author contributions: Conceptualization, methodology, materials processing and fabrication of testing specimens, planning and performing experiments, data analysis, visualizations, and writing original draft.

Paper B Prashant Gangwani, Janez Kovač, Nazanin Emami, Mitjan Kalin. (2024)
Effect of multi-scale fillers on the tribological behavior of UHMWPE composites in water-lubricated contacts.
Tribology International (Elsevier)
DOI:10.1016/j.triboint.2024.109669
Author contributions: Conceptualization, methodology, materials processing and fabrication of testing specimens, planning and performing experiments, data analysis, visualizations, and writing original draft.

Paper C Prashant Gangwani, Nazanin Emami, Mitjan Kalin. (2025)
Tribological behaviour of nano-titanium dioxide filled UHMWPE composites with a variety of micro fillers based on carbon, boron nitride and silicon dioxide under water-lubricated condition
Tribology International (Elsevier)
DOI: 10.1016/j.triboint.2024.110479
Author contributions: Conceptualization, methodology, materials processing and fabrication of testing specimens, planning and performing experiments, data analysis, visualizations, and writing original draft.

Paper D Prashant Gangwani, Nazanin Emami, Mitjan Kalin. (2025)
Role of fillers on the tribological behaviour of UHMWPE composites in environmentially acceptable lubricants. *(To be submitted)*
Author contributions: Conceptualization, methodology, materials processing and fabrication of testing specimens, planning and performing experiments, data analysis, visualizations, and writing original draft.

CONFERENCE CONTRIBUTIONS

Prashant Gangwani, Nazanin Emami, Mitjan Kalin. Influence of filler combination and scale on tribological performance of UHMWPE composites under water lubricated condition. (Poster Presentation)
SLOTRIB 2024 : Posvetovanje o tribologiji, mazivih in zelenih tehnologijah
10. junij 2024, Portorož.

Prashant Gangwani, Nazanin Emami, Mitjan Kalin. Investigating the role of a hard nano-filler on the tribological performance of multi-scale UHMWPE composites under water-lubricated condition. (Oral Presentation)
PolyTrib 2024 : 5th International Conference on Polymer Tribology
3rd - 4th October 2024, Portorož, Slovenia.

Prashant Gangwani, Nazanin Emami, Mitjan Kalin. Investigating synergism potential of graphite and boron nitride fillers for enhanced tribo-performance under aqueous condition.
Tribology for a sustainable and resilient future : 48th Leeds-Lyon Symposium on Tribology.
5 - 7 September 2023, Leeds, UK.

ACRONYMS

	Full Form
BC	Boron Carbide
BMI	Bismaleimide
CNT	Carbon Nanotube
COF	Coefficient of Friction
EP	Epoxy
h-BN	Hexagonal Boron Nitride
KT	Potassium Titanate
MAH	Maleic Anhydride
MoS_2	Molybdenum Disulfide
MWCNT	Multi-Walled Carbon Nanotube
PA6	Polyamide 6 (Nylon 6)
PA66	Polyamide 66 (Nylon 66)
PAH	Polycyclic Aromatic Hydrocarbons
PAI	Polyamide-imide
PC	Polycarbonate
PEI	Polyetherimide
PEEK	Polyether Ether Ketone
PI	Polyimide
POM	Polyoxymethylene
PPS	Polyphenylene Sulphide
PSU	Polysulfone
PTFE	Polytetrafluoroethylene
PU	Polyurethane
SCF	Short Carbon Fibre
SGF	Short Glass Fibre
Si_3N_4	Silicon Nitride
SiC	Silicon Carbide
SiO_2	Silicon Dioxide
SQF	Short Quartz Fibre
TiO_2	Titanium Dioxide
UHMWPE	Ultra High Molecular Weight Polyethylene
WS_2	Tungsten Disulphide

CONTENTS

LIST OF FIGURES

LIST OF TABLES

Part A. Comprehensive Summary

CHAPTER 1

Introduction

1.1 Background

Friction and wear in water-based systems, such as marine propulsion systems, hydropower turbines, and industrial pumps, result in staggering energy losses and maintenance costs worldwide. Studies estimate that friction-related energy losses in marine propulsion systems account for approximately 15–20 % of the total energy produced from fuel consumption [1,2]. However, the concern extends beyond unused energy. According to a report by the European Commission, large vessels such as container ships and oil tankers contributed to 4 % of total CO_2 emissions from the transport sector in 2023 [3,4]. This equates to nearly 140 million tonnes of CO_2 emissions annually, solely due to friction losses in international shipping, based on 2023 data [5]. In the case of hydropower turbines, although overall energy losses are lower compared to propulsion systems, wear-induced inefficiencies gradually reduce energy output, leading to costly repairs and downtime [6,7]. Similarly, statistics suggest that approximately half of all failures in centrifugal pumps are attributed to rolling bearing. However, even before complete failure, the defects in bearings can lead to an 20 % increase in power consumption [8,9]. These figures underscore the need for advance materials that minimize friction in water-based environments while sustaining operational efficiently for decades.

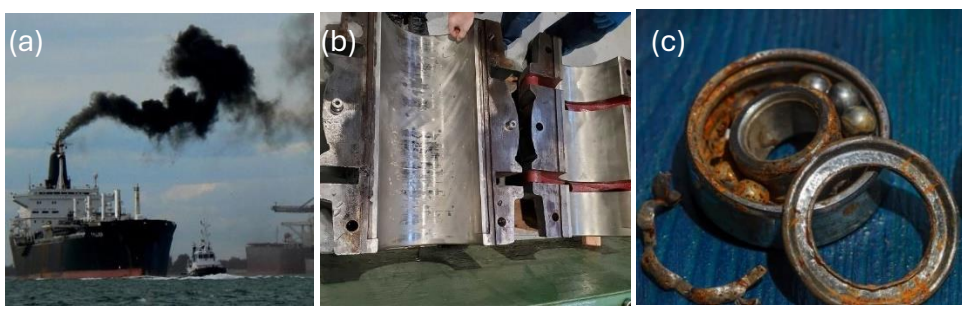

Figure 1 – (a) Emission from ships [10], (b) Damaged thrust bearing from hydro-turbine [11], (c) Failed roller bearing from pump [12]

1.2 Problem with conventional lubricants

Conventional oil-based lubricants, while effective in reducing friction, pose significant environmental risks when used in water-based systems. Annually, approximately 20 million tonnes of lubricants are estimated to leak into ecosystems through spills, discharges, or evaporation [13]. While exact figures vary between sources, all estimates indicate that millions of tonnes of lubricants are unintentionally discharged into oceans each year, primarily through operational leaks, improper disposal, and bilge water emissions from ships [14,15]. These lubricants contain polycyclic aromatic hydrocarbons (PAHs), which accumulate in plankton, fish, and other aquatic organisms, impairing reproduction and survival rates [16]. Studies suggest that even low concentrations of PAHs (0.45 μg/L) can induce morphological defects in marine species and disrupt food chains [17]. Furthermore, the remediation of oil-polluted water is costly and complex. Mechanical recovery methods for marine oil spills reclaim only 40% of spilled oil, while bioremediation (relatively eco-friendly) requires months to years to degrade contaminants and incurs expenses exceeding tens of thousands of euros per tonne [18,19].

Figure 2 – (a) Oil spill near coral atoll in the south pacific [20] and
(b) Contaminated river in Manipur, India after oil leak from power plant [21]

Biodegradable lubricants, such as vegetable oil and synthetic ester-based lubricants, are often promoted as sustainable alternatives, but they also have limitations. Firstly, the cost of these alternatives is typically two to three times higher than that of conventional oil-based lubricants, making widespread adoption challenging [22,23]. Even so the vegetable oil is considered unsuitable for use in highly saline environments as it may accelerate hydrolysis reactions [24], in-turn breaking the ester bonds in oils' molecular structure. This oil with compromised structure then has lower lubricity property than it should. Moreover, while the above lubricants contain lower PAH content, their degradation byproducts (such as acids and ketones) are water-soluble and can still exhibit toxicity in aquatic ecosystems. Studies imply the water-soluble fractions of oxidised lubricants can cause morphological defects in aquatic life [17,25]. These drawbacks highlight the need for lubricants that are safe for use in water-based

environments while capable of delivering lubricating performance with minimal compromise.

1.3 Water and water-based lubricants as an alternative

Water emerges as ideal lubricant for such applications, offering inherent advantages. In places like the marine environment where water is readily available in abundant quantity, its use as a lubricant reduces the need for lubricant storage or transport. Additionally, having pure water as a lubricant (without additives) eliminates the risks of bioaccumulation and marine pollution. Moreover, the high heat capacity of water reduces thermal degradation risks in high-load scenarios, while its fire-resistant properties enhance safety in industrial pumps and turbines.

Both the available results and computational fluid dynamics simulations suggests that in high-speed applications water's low viscosity enhances fluid film formation and has suitably low coefficient of friction [26,27]. However, the same low viscosity (1/100th that of oil and decreases rapidly further with temperature [26]) also implies that water-lubricated contacts in most cases will spend a higher portion of their operating cycle in boundary & mixed lubricated regime. Since surfaces in these regimes are in full or partial contact, wear of the surfaces is expected to occur throughout the operation cycle in water-lubricated contacts. This necessitates the development of advanced materials to use with water-lubrication that exhibit extremely low wear rates and are highly resistant to corrosion.

Operating in boundary and mixed lubrication regimes is not necessarily a disadvantage, as in many cases the solid lubricants are observed to have no effect after the system transitions to the hydrodynamic lubrication regime. For instance, Figure 3 delineates the effect on coefficient of friction with sliding speed from having graphene as a filler in the poly alpha olefin (PAO) oil in a steel–diamond-like carbon (DLC) contact. At lower sliding speeds, the incorporation of graphene in the lubricant is noted to reduce the coefficient of friction, with higher graphene concentrations leading to a lower coefficient of friction. However, at high sliding speeds—implying that the contact conditions are transitioning towards mixed and hydrodynamic regimes—the coefficient of friction is noted to be the same, irrespective of the presence or absence of graphene as a filler or its concentration. This is because in mixed and hydrodynamic conditions, the lubricant properties play the key role in determining the coefficient of friction, whereas in boundary conditions both lubricant and surface characteristics play a substantial role. This obervation underscores the advantage of operating in boundary regime when using lubricant like water.

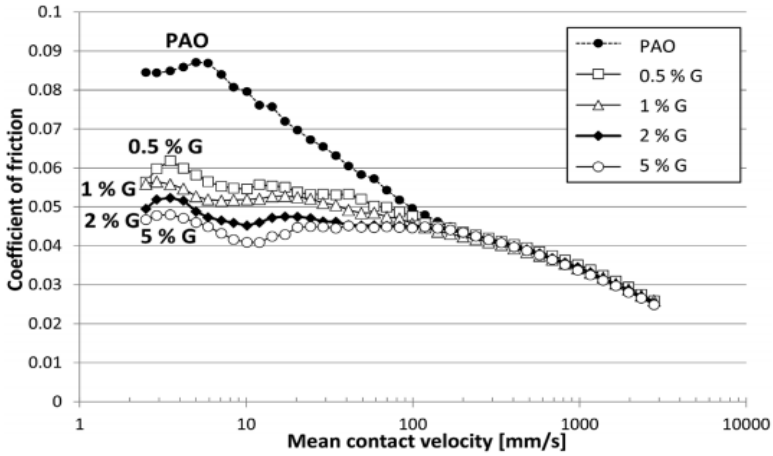

Figure 3 – Variation of Coefficient of friction with velocity with poly alpha olefin oil (PAO) containing different concentrations of graphene (G) [28].

Polyhydric alcohols, such as glycerol, present another promising alternative for water-based tribological systems. Glycerol, a non-toxic and biodegradable compound, forms hydrogen-bonded networks with water, increasing viscosity and thermal stability without the oxidative instability seen in vegetable oils [29,30]. Molecular dynamics simulations reveal that in comparison to pure water, having glycerol-water mixture as lubricant significantly improve its ability to remain between surfaces and reduces density fluctuations, thus enabling more stable lubrication film to form between surfaces [31,32]. This is critical for applications operating across variable temperatures, where glycerol's cryoprotective properties may prevent ice nucleation, thereby reducing mechanical stress in machines during cold starts [33]. Furthermore, multiple studies demonstrate that glycerol-water mixtures exhibit lower coefficients of friction and reduced wear volumes compared to conventional mineral oils as lubricant [34–36]. Additionally, glycerol's hydroxyl-rich structure is observed to be effective in passivating metal surfaces, thereby hindering corrosion of the surfaces [37–39], which can be a major concern when using water as a lubricant. Finally, since glycerol is the primary byproduct from biodiesel production, the existing infrastructure makes production of glycerol more economically viable than other synthetic lubricants [40]. These advances highlight the feasibility of integrating glycerol with water for use as lubricant as it presents promising compromise between ecological safety and performance reliability in water-based applications.

1.4 Polymer-metal contacts for water-lubricated conditions

Polymers are known for their self-lubricating properties, corrosion resistance, among other advantages delineated in Figure 4, making them a promising candidate for water-lubricated applications.

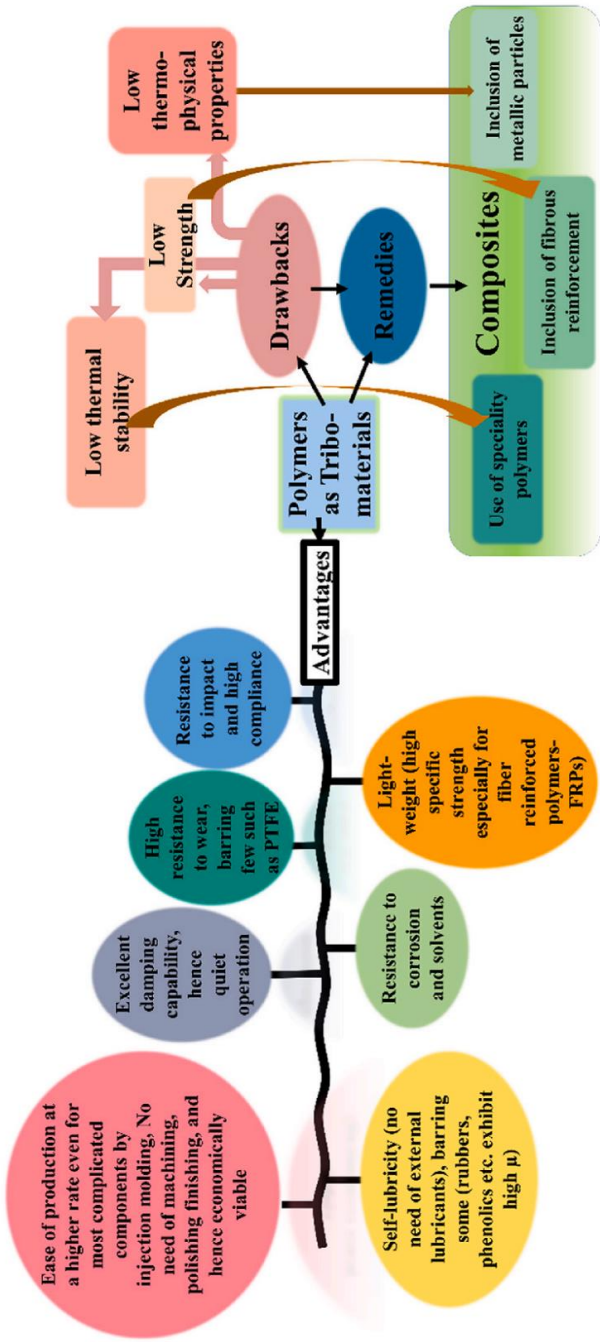

Figure 4 – Advantages and drawbacks of using polymers as tribo-materials [41]

1.4.1 Classification of polymer materials

A variety of materials are available for use, as shown in Figure 5. The easiest classification between these polymers is thermoplastics, thermosets and Elastomers.

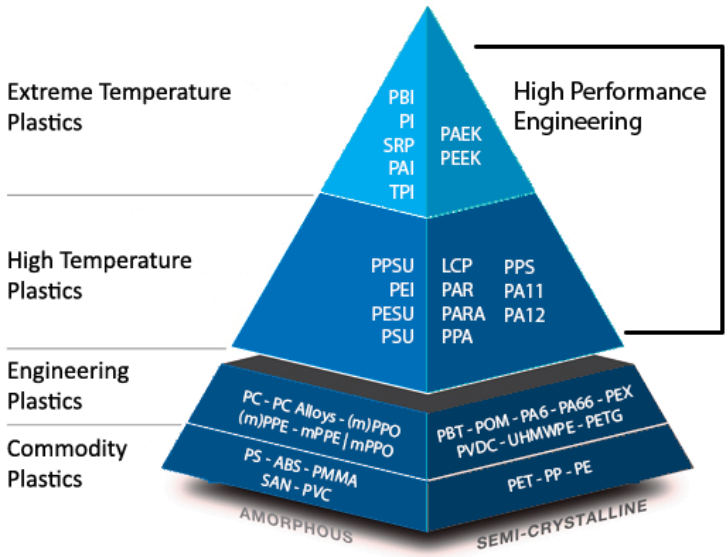

Figure 5 – Classification of polymers based on semicrystalline and amorphous [42]

Thermoplastics are polymer materials with ability to be remelted and reshaped, making them recyclable and suitable for applications requiring repeated processing. Thermoplastic polymers can be further classified as semi-crystalline or amorphous, depending on their molecular arrangement. Semi-crystalline thermoplastics have an ordered molecular structure with a sharp melting point and remain solid until a specific amount of heat is absorbed. They offer good chemical resistance and show significant improvement in heat deflection temperatures when reinforced, maintaining useful strength and stiffness well beyond their glass transition temperature (Tg). Examples of semi-crystalline thermoplastics include Polytetra- fluoroethylene (PTFE), Ultra-high-molecular-weight polyethylene (UHMWPE), Polyoxymethylene (POM), Polyphenylene sulfide (PPS), and Polyether ether ketone (PEEK). On the other hand, amorphous thermoplastics have a randomly ordered molecular structure and do not have a distinct melting point. Instead, they soften gradually over a temperature range. These have lower mould shrinkage, making them ideal for precision applications. However, amorphous thermoplastics typically lose strength more rapidly above Tg. Common amorphous thermoplastics include Polycarbonate (PC), Polysulfone (PSU), and Polyetherimide (PEI).

Thermoset polymers undergo an irreversible curing reaction that forms a highly crosslinked molecular structure, preventing them from being remelted or reshaped after curing. This crosslinking results in exceptional thermal stability, mechanical strength, and chemical resistance, making thermosets ideal for high-performance applications such as aerospace, automotive, and electronic components. Unlike thermoplastics, thermosets do not soften upon heating; instead, they degrade or char at high temperatures. While some thermosets may exhibit an amorphous molecular structure, others develop ordered regions during crosslinking. Thermosets also generally have low mould shrinkage and high dimensional stability. However, they are more brittle than thermoplastics and cannot be recycled due to their permanent crosslinked structure. Some well-known thermosetting materials include Epoxy resins, Polyimide (PI), Polyamide-imide (PAI), Phenolic resins, and Bismaleimide (BMI).

Elastomers, on the other hand, are unique class of polymers characterized by their exceptional viscoelastic behaviour (combining both viscosity and elasticity), allowing them to undergo significant deformation and return to their original shape with minimal energy loss. Elastomers can be categorized into thermosetting and thermoplastic elastomers. Classic thermoset elastomer examples include natural rubber, neoprene (polychloroprene), and vulcanized styrene-butadiene rubber (SBR), which are form through irreversible curing, creating permanent crosslinks. Depending on crosslink density, chemical makeup and saturation, these vary in temperature and chemical resistance. In contrast, thermoplastic elastomers such as styrenic block copolymers (SBCs), thermoplastic polyurethane (TPU), thermoplastic vulcanizate (TPV), and thermoplastic polyolefins (TPOs) can be melted and reshaped multiple times without significant loss of properties.

The mechanical properties vary significantly among polymers, even when belonging to similar classification (see Table 1). Additionally, with variety of options available the selection of appropriate matrix material for a specific application could become a complex task. Luckily, reasonable research is available on virgin polymers against metal in water-lubricated conditions, making it easier for selecting the correct matrix materials.

Table 1: Mechanical Properties and other characteristics of various polymers [43,44]

Polymer	Density (g/cm^3)	Hardness	Tensile Strength (X 10 MPa)	Izod Impact Strength (X 10 J/m)	Elastic modulus (GPa)	Water Absorption (%) 24h at 23°C	Elongation (%)	Continuous service temperature (°C)
PA6	1.06-1.16		7-10	6-16	0.8-3.8	7.1-10	10-160	
UHM-WPE	0.93	57-68 (M)	2-5	>85	0.7-0.9	0.01-0.02	250-600	82
POM	1.49-1.53	79-92 (M)	5-6	6-12	2.4-3.2	0.80-1.65	20-120	90
PPS	1.42-1.44	90-95 (M)	9	0.2-0.3	3.8	0.01-0.03	3-8	< 240
PEEK	1.38-1.40	120 (R)	7-10	7-9	3.5-4.0	0.10	20-50	260
PAI	1.38-1.42	86-127(E)	15-20	13-14	4.4-4.9	0.33	15-35	260
PI		112 (M)	8-24	4-11	1.2-3.8	0.39-2.90	7-95	250-300

1.4.2 Tribological performance of neat polymer against metal

Golchin et al. conducted one of the most extensive studies comparing the tribological performance of various thermoplastic polymers [45]. Among them, polytetrafluoroethylene (PTFE) and ultra-high-molecular-weight polyethylene (UHMWPE) exhibited the lowest coefficients of friction, making them attractive choices for matrix materials. However, PTFE demonstrated extremely high wear rates compared to other polymers, reducing its suitability. Conversely, UHMWPE, while second in terms of low friction, exhibited the lowest wear rate, making it the most favourable option overall.

Another promising material is polyphenylene sulfide (PPS), which has a coefficient of friction of 0.33 and a wear rate of 6×10^{-4} mm^3/Nm under conditions similar to Golchin et al. aforementioned study [46]. However, PPS is inherently brittle (as observed in Table 1), necessitating fibrous reinforcement or blending with other polymers for improved mechanical properties.

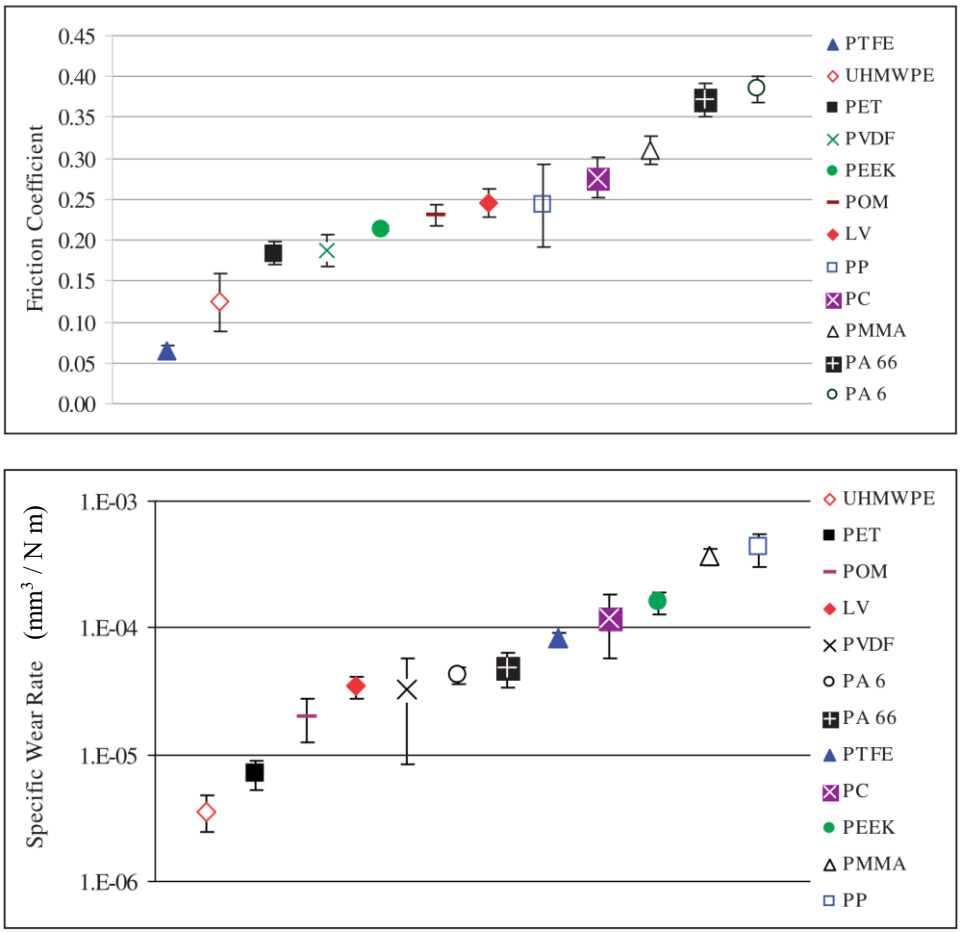

Figure 6 – Comparison of tribo-performance of various polymer materials in water lubrication (5 MPa, 0.13 m/s) [45]

Meanwhile for thermosetting polymer such as polyimide (PI), studies with identical conditions were not found, making it difficult to compare with above materials. However, available studies indicate a relatively high coefficient of friction in the range of 0.25–0.30 [47,48], making it rather unfeasible option.

Tanaka [49] and Evans [50] observed that introducing water as a lubricant in polymer-metal contacts generally reduces the coefficient of friction but can also lower the wear resistance of the polymer. Another key observation from Tanaka was that the amount of transferred polymer in water-lubricated contacts was similar to that in dry sliding. Further it was suggested that the increased wear in water-lubricated conditions might be due to surface modification of the polymer by water rather than modification of the countersurface by polymer transfer. However, many studies contradict the above

and suggest that formation of the beneficial transfer film onto the countersurface is hindered in water-lubricated contacts. Moreover, increase in wear rate is not always observed upon incorporation of water as lubricant; it is highly dependent on the polymer itself and the operating conditions [51–55]. To understand why outcome differs in water-lubricated conditions even when surfaces are mostly in contact i.e., in boundary lubrication, we need to examine their lubrication mechanisms and failure.

1.4.3 Mechanism of polymer in water lubricated sliding

The presence of water brings the basic benefits of having any lubricant in a contact, as mentioned in Figure 7 (left). The melting of polymers due to increased temperature at the contact zone is a key limitation in dry sliding, but this concern is mitigated when water is present, as the lubricant acts as cooling agent. As a result, materials should theoretically be capable of operating at higher loads and velocities without failure. However, this also renders the concept of the 'PV limit' (which assesses polymer applicability based on frictional heat generation as a product of the coefficient of friction, pressure, and velocity) less relevant. When water is introduced, increasing velocity shifts the lubrication regime towards the right side of the Stribeck curve, increasing surface separation and reducing the real contact area. Furthermore, in many cases, frictional heat plays a crucial role in lubrication mechanisms, such as aligning short fibres, melting glass fibres to coat countersurfaces, or influencing the behaviour of wear debris [56,57]. Consequently, friction and wear mechanisms in water-lubricated sliding often differs from that in dry sliding.

The incoporation of water also brings several negative effects in polymer metal contacts. For instance, in dry polymer-metal contact, the polymer transfer layer on the metal acts as an effective lubricant. However, in water-lubricated conditions, this transfer layer is generally absent. Since surfaces like steel are hydrophilic i.e., they can be wetted by water; the water molecules can easily fill the surface cavities and then exclude any polymer from these cavities by hydraulic effect. Water (as a fluid) can also remove the worn material from the contact region and thereby avoid any accumulation of the worn polymer debris on the surfaces and hence denying the beneficial transfer layer formation on the metal surface.

However, some polymers, such as PPS, exhibit signs of physical transfer-layer on the metal surface even in the presence of water [46,51,58]. PPS has been observed to form a thin polymer transfer layer on the metal surface. In some cases, it also creates an inorganic chemical film on the countersurface, which can further enhance friction performance. However, the physical transferred layer is suggested to play the dominant role in all studies.

Additionally, water interacts with the polymer through absorption and penetration in several ways, the major ones being mentioned in Figure 7 (right) and elaborated in detail in the following text:

- ➔ *Plasticisation*- absorption of water molecules by the polymer surface and entering the bulk can soften and plasticise the polymer matrix, affecting its mechanical properties. This is a diffusion-controlled process and hence dependent on polymer, time, stress, temperature.
- ➔ *Prevention of worn polymer debris reattachment*- as the temperatures are kept low by water. Additionally, water flow removes debris from the contact area, further hindering transfer layer formation on metal surface. Some rolled and flattened debris do attach back to polymer trapping the water inside.
- ➔ *Surface swelling*- absorption of water leads to alterations in polymer structure at surface level. This alters the polymer material's elastic modulus and strength, which in turn affects its friction and wear behaviour.
- ➔ *Reduction in shear strength*- water absorption by polymer material can also lead to reduction in shear strength, potentially increasing its wear rate. However, this could also accelerate the initial formation of polymer transfer layer on the metal surface if the polymer is already plasticised before tribological testing.
- ➔ *Filler removal in composites*- In composite materials, water penetration can weaken the interface between the fillers and polymer matrix, leading to their removal and consequently increasing the wear rate.

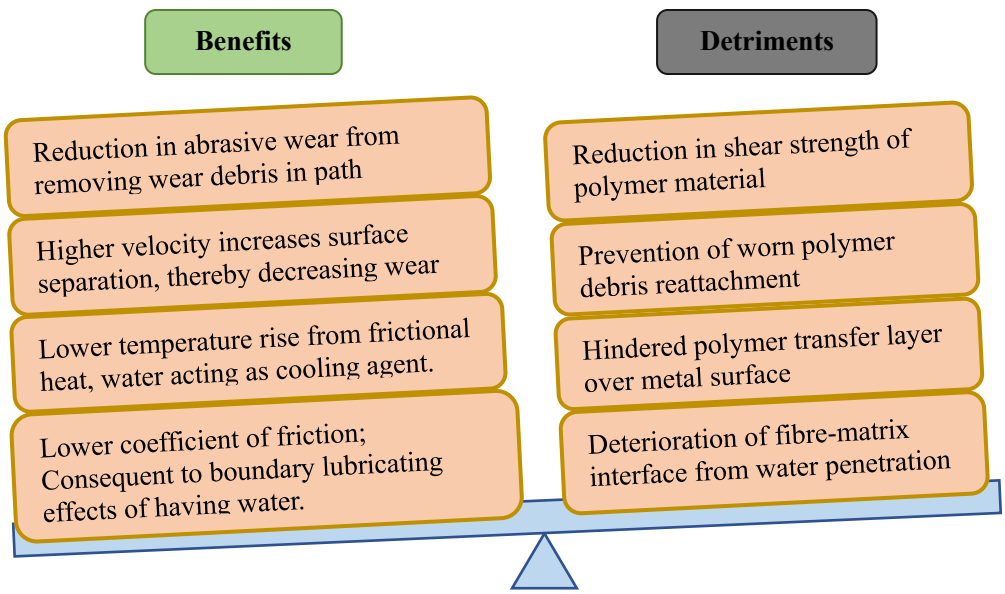

Figure 7 – Benefits and Detrimental effects of incorporating water in Polymer-Metal Contacts

1.4.4 Drawback of using neat polymer

The review of available studies has shown that polymers such as ultra-high-molecular-weight polyethylene (UHMWPE), polytetra- fluoroethylene (PTFE) and polyphenylene sulfide (PPS) exhibit excellent tribological performance under water-lubricated conditions. However, their use as neat materials in real-world applications is limited by several inherent drawbacks.

The key drawbacks (among others shown in Figure 4) include:

- For many practical applications, a material must not only provide low friction but also sufficient load-bearing capacity, a requirement that neat polymers often fail to meet. The neat polymers generally have low strength as see Table 1.
- The tribological performance of neat polymers under aqueous conditions is generally inferior to that achieved with oil-based lubricants. Not only a lower coefficient of friction is noted with oil-based lubricants, the formation of a stable hydrodynamic lubricating film also leads to lower wear rate of the surfaces [59].

This necessitates taking remedial actions such as inclusion of fibrous reinforcements and other fillers into the polymer. Consequently, the focus has shifted from the use of neat polymers to the 'polymer-composites', whose performance is of greater interest for real-life applications.

1.5 Fillers and additives into polymer matrix

Research has demonstrated that reinforcing polymers with fibres can improve their mechanical properties, while the inclusion of particulate fillers into the polymer matrix can enhance the tribological performance. However, these fillers come with their own set of drawbacks and adverse effects that are not encountered with neat polymers. Moreover, the introduction of water can also add to adverse effects in case of some fillers. For example, molybdenum disulfide (MoS_2) and tungsten disulfide (WS_2) can, under selective conditions, react with water to form acidic products [60,61]. Consequently, in this section we will look at the ambivalent effects from having fillers and possibility of using additives to counter them.

1.5.1 Fibrous reinforcements

The main purpose of fibrous reinforcements is to carry loads far excess of what the polymer matrix can support on its own. If the adhesion between the polymer matrix and fibre is good, the fibres bear the majority of load, resulting in significant improvement in overall strength of the material. Table 2 shows the comparative strength of several reinforcement materials. As observed, many of the reinforcement materials have properties comparable or even exceed that of certain steels while still weighing only a fraction of it. This means compared with traditional metal stuff like steel, the reinforcement materials can carry a higher load for a given weight.

Additionally, the melting temperature of these reinforcement materials is extremely high [62,63] so they do not suffer the same drawback as the polymer-matrix.

Table 2: Strength of various engineering fibers [64,65]

Material	Strength (GPa)	Modulus (GPa)	Density (g/cm^3)
Carbon	3.5	230	1.75
E-glass	3.4	150	2.6
p- Aramid	2.8	109	1.45
m-Aramid	0.85	17	1.38
Steel	2.8	200	7.6

Effect of fibrous reinforcements on tribological performance

Fibrous reinforcements are observed to provide different influences in dry and water-lubricated sliding. Hanmin et al [66] pointed the beneficial and detrimental effects of incorporating water in fibre-reinforced composites. The beneficial effect of water includes removing the generated frictional heat and considerably reduce temperature. Therefore, the deterioration of mechanical properties (such as strength and rigidity) in the contact region due to temperature rise is reduced. Another beneficial effect of having water lubrication is it facilitates removal of debris from the sliding region. This reduces the abrasive wear and in-turn enhances the polishing effect by fibres on the metal surface. The resulting decrease in surface roughness contributes to reduction in wear. On other hand, detrimental effects of having water include corrosion of fibres and worsened fibre-matrix interface from water penetrating the polymer. Table 3 summarises the advantages and drawbacks of using different fibres on tribological performance.

Table 3: Advantages and Drawbacks of using fibers in composites [41]

Fiber	Advantages	Disadvantages
Carbonaceous Carbon	Highest Strength, self-lubricity, efficient in film transfer, effective in friction and wear reduction	Disadvantageous in abrasive wear mode; Cost
Organic Fiber Aramid	Good strength and wear resistance (even in abrasive mode), Highest impact strength	No self-lubricity, low thermal conductivity, and moderate thermal stability
Ceramic Fibers Glass	Good Strength and moderate resistance to abrasion, low cost	No self-lubricity, increases friction, moderate thermal stability

Among the commonly used reinforcements, carbon fibres exhibit the greatest potential for enhancing the tribo-properties of polymer composites in water-lubricated condition. Their superior performance is due to the passivation of the dangling covalent bonds by adsorption of water during the wear process which enables maintaining low friction [67] while simultaneously enhancing the mechanical and wear-resisting characteristics of the polymer composites. Compared to composites containing glass (SGF) or quartz fibre (SQF), the short carbon fibre (SCF) reinforced polyimide (PI) composites were observed to have better mechanical and tribological properties [47]. SCF-PI composites showed lower friction and wear characteristics under both dry and water-lubricated conditions. Meanwhile, the SGF or SQF containing composites were observed to be more susceptible to abrasion and breakage of fibres during sliding against metal in water-lubricated conditions. The transfer of broken fibres onto the metal surface increased its roughness which was designated as the main cause for increase in wear rate of the composite. Similar results have been reported with epoxy composites (EP) reinforced with SCF and SGF [68]. The surfaces obtained from test against composites reinforced with SCF exhibited significantly reduced abrasive wear and had signs of physical tribo-film present over the metal surface, whereas surfaces from composites reinforced with SGF endured severe scratching (owing to the high abrasiveness of SGF). As a result, the formation of physical tribo-film over metal surface was inhibited for SGF composites especially ones without sold lubricants.

Moreover, the constituents of glass fibre (SiO2) produce hydroxides and hydrates in water. The mechanical strength of these is lower than SiO2 [38–40], which might be another reason why glass fibre exhibit poor wear resistance compared to carbon fibre in water-lubricated condition. Additionally, because water alleviates the temperature rise at the contact region, short glass fibres do not melt to form a lubricating layer over the metal surface-as is sometimes observed in dry sliding conditions [56].

Issues with fibrous reinforcements

Although incorporating fibrous reinforcements allows the resulting composite to withstand higher loads and reduces wear relative to neat polymers, it can also introduce new challenges. In highly non-polar matrices such as UHMWPE, the interaction between the polymer and reinforcement fibres is often suboptimal (see Figure 8).

Moreover, the above not only diminishes the anticipated benefits of fibre reinforcement but can also adversely affect the performance of other fillers within the matrix. For example, Golchin et al. [46] investigated having SCF, graphite and multiwall carbon nano tubes (MWCNT) in PPS matrix under distilled water lubrication. They observed that the addition of either MWCNT or graphite did not improve the wear resistance of SCF reinforced PPS composite. The weakening of interfacial bonds between the fibre and matrix was attributed as the reason for this. The weakened interfacial bonds led to easy removal of thinned and broken fibres, which consequently increased the wear rate of the composite.

A potential strategy to address this issue involves either treating the individual components to increase their polarity or introducing another component, a compatibilizer, whose primary function is to mediate the interaction between the original components.

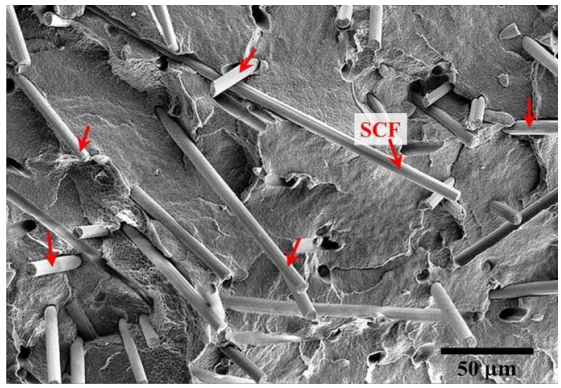

Figure 8 – Interface between short carbon fibres and UHMWPE observed in composite [72]

1.5.2 Compatibilizers

Compatibilizers are molecules that contain highly polar functional groups, enabling them to form physical and chemical bonds with polymer chains and other composite components, thereby acting as chain extenders or adhesion improvers as can be seen in Figure 9.

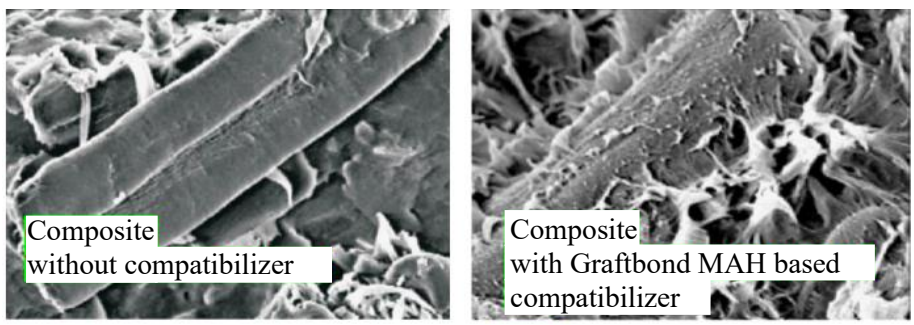

Figure 9 – Scanning electron images showing status of polymer material around carbon fibre in absence (left) and presence (right) of maleic anhydride based compatibilizer. [73]

The above action not only abates fibre pullout but also improves the overall mechanical properties of the composite. Karsli et al. [74] observed that the incorporation of a small concentration of maleic anhydride (MAH)-modified polypropylene (PP) as a compatibilizer increased the tensile strength of the composite by approximately 30 % compared with a composite lacking a compatibilizer (see Figure 10a). A similar increase in hardness was also noted. Lv et al. [75] on the other hand incorporated the MAH grafted compatibilizer to nylon 1212 reinforced with MWCNT and observed the variation in impact strength. The results showed a significant improvement in impact strength (upto 4 times) in presence of compatibilizer (see Figure 10b).

All the above suggest that compatibilizers not only help address issues such as fibre pullout but can also contribute to overcoming inherent drawbacks of materials such as low impact strength in case of PPS (which is a critical issue when using material in real-world applications).

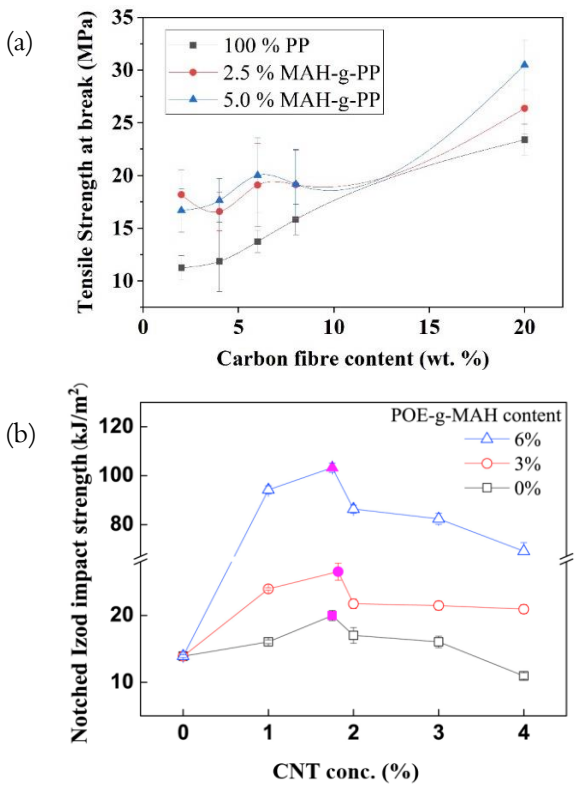

Figure 10 – (a) Variation of tensile strength in carbon fiber reinforced PP composites with the incorporation of MAH-g-PP as compatibilizer [74] (b) Variation of impact strength of PA composites containing MWCNT upon the incorporation of POE-g-MAH as compatibilizer [75]

1.5.3 Fillers for improving tribo-performance

For ease of understanding and how fillers work to improve tribological performance composite metal / contacts, we can classify fillers into 'soft' and 'hard/strong'.

➔ Interface modification: The composites here consist of a soft filler dispersed in a hard, strong matrix. Soft fillers, such as PTFE and graphite, exhibit superior lubricity (i.e. a lower coefficient of friction) due to their low shear strength, while the strong matrix, for example PEEK or epoxy, provides high wear resistance. Initially when composite meets the metal surface, see Figure 11 (1a), high coefficient of friction (COF) is encountered, and the asperities metal the metal wears off the matrix. No matter how sturdy the matrix polymer is, its strength is still quite low compared to metal countersurface. Consequently, the wear of polymer will occur however the wear rate will be significantly less compared to if the soft filler material was used as a matrix. The worn matrix material fills the dips in the countersurface trying to form a transfer film. With the removal of matrix by countersurface asperities, there comes a time when fillers (present inside composite) start to expose Figure 11 (1b). The sliding motion between the polymer and metal has shearing stress on these exposed fillers. Since these fillers have low shear strength, they get easily sheared off and start forming their film together with the one with matrix Figure 11 (1c). When sufficient fillers have been exposed & sheared upon the continuous wearing of a matrix, the film gets thicker and protects above unworn composite from the countersurface asperities. Since fillers possess better lubricating properties, the observed friction is lower than that with only a matrix. The main requirement for this is the availability of the fillers in sufficient amounts at the interface for a noteworthy reduction in coefficient of friction to happen. The main disadvantage is the reduction of strength and load-carrying capacity of the composite compared to the matrix material.

➔ Bulk modification: The wear properties of excellent self-lubricating polymer matrix such as PTFE can be improved by adding hard or strong filler materials (particles or fibres). The filler here can be metals or ceramics, for example Titanium dioxide (TiO_2), potassium titanate (KT), etc., which have the strength to smoothen the metal countersurface if required. Similar to the previous case the polymer matrix fills the voids until fillers are exposed Figure 11 (2b). Upon exposure of fillers to the surface, they can provide surface smoothening action by ramming with the countersurface asperities Figure 11 (2c). Decrease in countersurface roughness means lower wear-causing effects such as ploughing. Once the surfaces are smooth enough the hard fillers roll between the two surfaces preventing the surfaces to contact each other ergo converting sliding into rolling Figure 11 (2d). The COF remains low or increases marginally but wear resistance increases significantly.

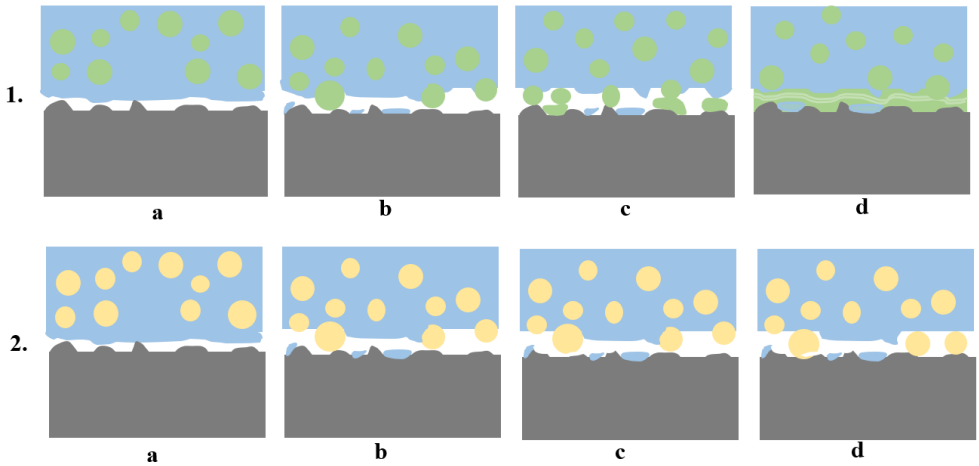

Figure 11 – General working mechanisms in 1. Interface and 2. Bulk Modification

Various particles have already been explored to be use as fillers in the polymer matrix under water lubricated conditions. In addition to the Interface and bulk modification mechanisms, certain fillers also react with water to provide an additional lubrication effect. However, the nature of this reaction is dependent on the filler and is best to discuss separately for each type. For ease these are going to be classified as carbonaceous and non-carbonaceous.

Carbonaceous filler as additive in polymer matrix

Graphite is a crystalline form of carbon known for its lubrication properties, resulting from its layered structure. The atoms are arranged in hexagonal sheets held together by strong covalent bonds within each layer, while weak van der Waals forces act between the layers as shown in Figure 12a. This allows the layers to slide over one another with minimal friction when subjected to pressure, making graphite a great solid lubricant. During sliding, defects are generated in the graphite structure which can be evaluated from observing the D and G bands from Raman before and after sliding [76]. In humid environments these defects are closed by different structures and the repulsive effect between these structures being responsible for the reduction in the coefficient of friction [77,78].

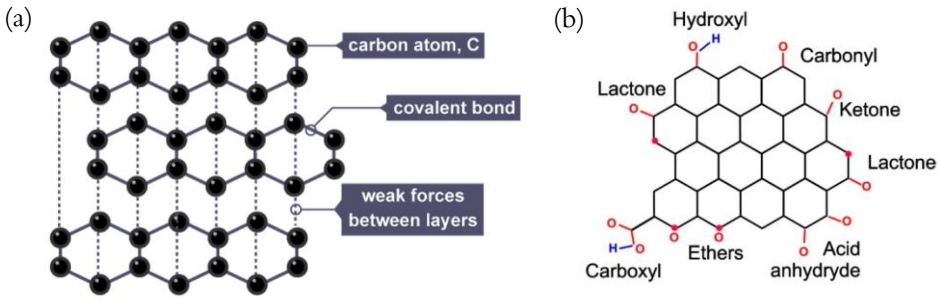

Figure 12 – (a) Structure of Graphite [79], (b) Possible functional groups closing the edge (in humid environment, hydroxyl is most possible to close defects) [80]

Various studies [46,68,81,82] have demonstrated that graphite is an effective microscale filler for water-lubricated conditions. It has been tested as filler in various polymer materials including PPS, and epoxy in the presence of distilled and tap water as lubricants. In both cases, introduction of graphite showed a reduction in the coefficient of friction. Additionally, graphite was observed to reduce the coefficient of friction even in presence of carbon fibre reinforce in the matrix [46]. Cui et al. [82] evaluated the performance of graphite and Ni coated graphite in seawater at various loads and speeds, concluding that graphite serves as an effective solid lubricant for friction reduction in seawater environments as well. From a concentration assessment, the two studies investigating the effect of concentration [46,82] indicated a high concentration of graphite (around 10 wt.%) yields a significant reduction in friction.

Non-Carbonaceous filler as additive in polymer matrix

Ceramics are inorganic, non-metallic materials that are brittle and hard in compression but comparatively weak in shearing and tension. They have been observed to improve the mechanical properties when incorporated in composites [83–85]. The ceramic particles that were observed to be effective and improved the performance with water-lubricated systems consist of both oxides (SiO_2, TiO_2) and non-oxides (SiC, Si_3N_4, hBN) [86–93].

Silicon dioxide (SiO_2) features a network of silicon and oxygen atoms as shown in Figure 13a that can form a protective layer on surfaces. This layer effectively reduces coefficient of friction and wear rates by creating a self-laminating film during tribological interactions. Under water lubricated conditions, it is observed that the low friction is a result of the dissolution and hydration of silicon dioxide. The hydration and dissolution products of silicon dioxide (shown in Figure 13b) smoothens the surface and increases the viscosity of water to promote hydrodynamic lubrication. However, less is known about the effects of surface modified hydrophobic silica particles on the tribological performance.

(a)

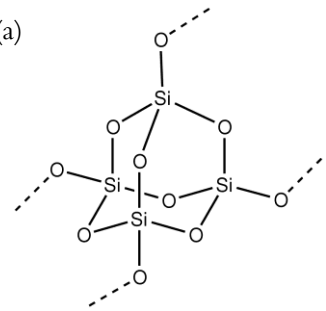

(b)

dissolution

$$SiO_2(s) + 2H_2O(l) \rightarrow H_4SiO_4(aq)$$

hydration

$$SiO_2(s) + 2H_2O(l) \rightarrow Si(OH)_4$$

Figure 13 – (a) Structure of silicon dioxide, (b) Reaction of silicon dioxide with water

Studies on using SiO_2 as a filler have reported both positive and negative outcomes. Song et al [94] investigated the possibility of using nano-SiO_2/PU coating in different lubrication mediums and observed that adding SiO_2 in PU matrix deteriorated the friction and wear performance at all concentrations. Additionally, the wear mechanism was observed to be abrasive in water-lubricated condition. In contrast, another study demonstrated that the addition of SiO_2 nanoparticles to phenolic laminates yielded ultra-low friction behaviour against 316 steel under water-lubricated conditions [86] (block-on-ring, 200 N, 0.5 m/s, pure water).

Hexagonal boron nitride (hBN) often referred to as "white graphite", possesses a layered structure similar to graphite as shown in Figure 14a. This allows its sheets to slide over one another easily, which results in excellent lubrication performance under high temperatures and pressures. Under water lubricated conditions however, studies indicate that hBN reacts with water to form diboron trioxide (B_2O_3), with further reaction leading to formation of a water-soluble product (H_3BO_3), as shown in Figure 14b. These reaction products are believed to form a protective layer on the surface, reducing wear while also providing additional lubrication.

Several studies have proven the effectiveness of hexagonal boron nitride (hBN) as both an anti-friction and anti-wear filler in distilled water and seawater environments [89–92]. However, its use as a filler in polymer matrix under water has been less extensively explored. Li et al. [89,90] investigated hBN as an filler in boron carbide (BC) under distilled water-lubrication. The hBN particles used were micron size and tribological characteristics were evaluated in a rounded-pin-on-disc configuration (10 N, 1.31 m/s) with the concentration of hBN varied from 0-30 wt. %. They observed a significant reduction in both friction (0.373 to 0.005) and wear rate ($1.5x10^{-5}$ to $0.15x\ 10^{-5}$ mm^3/Nm) with optimum concentration of hBN particles in both studies to be 20 wt. %. One study was noted where use of nano-sized hBN was explored as filler in carbon fibre reinforced POM matrix at various loadings in a block-on-ring arrangement under tap water lubrication [92]. Similar results delineating reduction in coefficient of friction and wear rate were again observed. In all the above studies, it was inferred that the formation of B_2O_3 protected the surface.

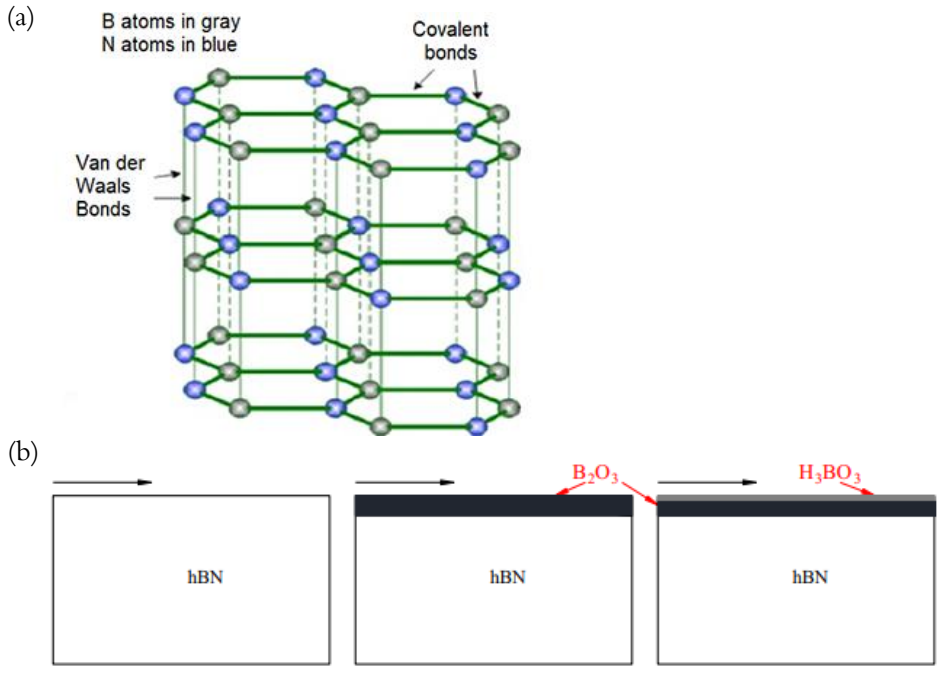

Figure 14 – (a) structure of hexagonal-Boron Nitride (h-BN) [95],
(b) Reaction products of h-BN with water [89]

Titanium dioxide (TiO_2) is another ceramic material that has been found to be effective under water lubricated conditions. Naturally, TiO_2 exists in three forms with structure shown in Figure 15. Among these, Rutile & Anatase are in more stable forms and easily available In terms of particle morphology, rutile particles are needle-shaped, whereas anatase particles are more rounded, making them more favourable as fillers [96]. Further, the anatase form is also more cost effective than rutile.

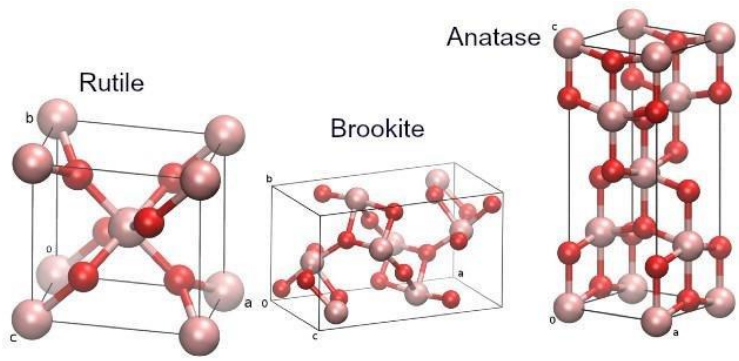

Figure 15 – Structures of different forms of Titanium dioxide available [97]

Kurdi et al [98] investigated the effect of concentration of nano-TiO_2 under dry and water-lubricated conditions. Tests were conducted on a pin-on-disc arrangement at 5 N load and 0.1 m/s for 24hrs against 100Cr6 steel disc. The results are shown in Figure 16. It was inferred that in dry conditions the lubricating performance was determined by the PEEK polymer with negligible contribution from the nanoparticles. With the incorporation of water, the wear of the PEEK matrix increased significantly due to the absence of the brittle-to-ductile transition, as water dissipates frictional heat. However, the deterioration in wear was minimized to a large extent by incorporating TiO_2. Having TiO_2 nanoparticles as filler reduced the coefficient of friction further and abated wear rate under water-lubricated sliding. Moreover, concentration of nanoparticle exceeding 5 wt.% did not yield further improvements in tribological performance, suggesting 5 wt.% to be the optimum concentration.

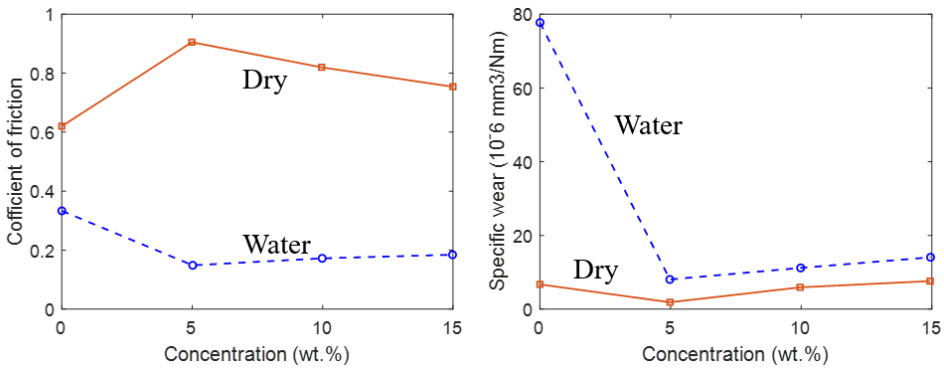

Figure 16 – Effect on coefficient of friction and wear performance for PEEK composites incorporating various concentration of nano TiO_2 against 100Cr6 steel in pin-on-disc arrangement under dry and water lubricated condition. (Data from [98])

Similarly, Li et al. [99] reported that having TiO_2 nanoparticles effectively reduced the wear rate and improved the vibration dampening in bearings made from UHMWPE designed for marine applications. Additionally, introduction of titanium dioxide as filler is known to improve the mechanical properties of composites [100,101], with the nano-scale particles providing superior improvements compared to micro-scale, even at a fraction of the concentration. The UHMWPE composites containing nano-scale titanium dioxide particles also have a better resistance to abrasive wear than their micro-scale equivalent [101,102].

It is observed from the literature survey that an effective way to obtain even lower coefficient of friction and wear rate is by incorporating multiple fillers into the polymer simultaneously.

1.6 Multiscale composites

Incorporating fillers of different scales into a polymer matrix might lead to significant improvements in tribological performance, provided the components interact synergistically. Additionally, when the fillers of different scales (micro and nano) are present the resulting material is then referred to as a 'Multiscale composite'. This tactic of employing several multiscale fillers in search for superior performance has been observed in studies under both dry [65,103,104] and water-lubricated [46,68,105–107] sliding.

For example, Gao et al. [68] observed this effect from having 3 wt. % nano-SiO_2 and 8 wt. % graphite in SCF reinforced epoxy. The tests were performed on block-on-ring arrangement with the rings made of water-resistant stainless steel and entire arrangement immersed in tap water. Tests were conducted with varying speeds from 0.1 to 3 m/s and a constant load of 100 N. They observed the incorporation of nano-SiO_2 into the graphite-containing epoxy proved beneficial in lowering the coefficient of friction and wear rate across all test parameters.

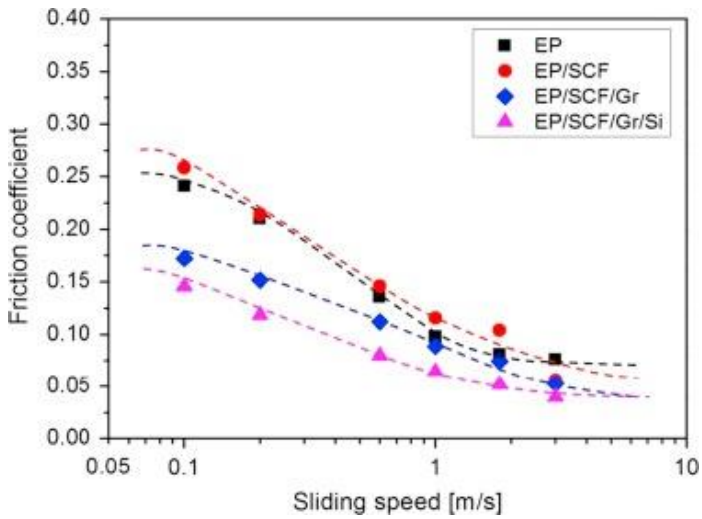

Figure 17 – Variation of coefficient of friction with sliding speed for neat epoxy and composites containing different filler combinations tested against stainless steel in block on ring arrangement. [68]

Similarly, Chen et al.[107] explored the possibility of synergism between graphite and carbon nano tubes (CNT) under sea-water lubrication. Initially, the optimum concentration fillers were determined in the parent polymer, which turned out to be 10 wt.% for graphite and 5 wt.% for CNT respectively. Following which it

was observed that having both graphite and CNT in optimum quantities in a single composite led to further improvements in tribological performance. However, it was also noted that the incorporation of graphite did not improve the friction-related properties of the matrix. This was because the multilaminate structure of graphite was destroyed and transformed into much thinner layers, losing its self-lubricating qualities. However, the composite containing both fillers showed further improvement in friction and wear resistance compared to the composite containing only one filler, implying having additional filler may have somehow contributed to the functioning of graphite.

However, an improvement in tribological performance from introducing multiple fillers in the polymer is not always the case. This is because the incorporation of an additional filler may also hinder the performance of another filler, instead of working synergistically like observed in the previous study from Chen et al.[107]. A good example of this is a study from Golchin et al. [46] which similar Chen et al. also investigated the effect on tribological performance upon having graphite and multi-wall carbon nano tubes (MWCNT) as fillers in SCF reinforced PPS under distilled water lubrication. It was observed that introducing either MWCNT or graphite as the additional filler in SCF reinforced composite led to an increase in wear rate. The weakening of interfacial bonds between the fibre and polymer-matrix was attributed as the reason for this. The weakened interfacial bonds caused easy removal of thinned and broken fibres, which acted as 3rd body and moved wear mechanism towards abrasion, consequently increasing the wear rate of the composite. Therefore, it is important to understand how each

All the above highlights the importance of understanding the interactions between different fillers, as their incorporation has not always led to synergistic effects in tribological performance. However, relatively less research has examined how the presence of one filler influences the performance of another, especially under lubricated conditions.

1.7 Current issues and Research gaps

Based on all the aforementioned subsections, here are the current issues :

- ➔ Based on the available numbers for water-based application, there appears to be a need for advance materials that minimize frictional losses in these environments while sustaining operational efficiently for decades. (Sub-section *1.1*)
- ➔ Additionally, use of conventional oil-based lubricants in these applications pose environmental risks if these lubricants find way into the water table. Further, since the remediation of oil-based lubricants is expensive and even then, only part of it is recoverable, need for more environment friendly alternatives is needed. (Sub-section *1.2*)

➔ A feasible solution appears to be using water itself as the lubricant or a mixture of water-glycerol (Sub-section *1.3*). Having water as lubricant, makes polymers particularly suitable as material due their self-lubricating and corrosion resistance properties (Sub-section *1.4*).

➔ Although neat polymers against steel are capable of providing decent coefficient of friction under water lubrication (Sub-section 1.4.2), they also pose several drawbacks (Sub-section *1.4.4*), requiring the need of polymer-composites.

➔ The current status of work in the field of polymer-composites suggests that simultaneous incorporation of several reinforcement, fillers, and additives, has potential to solve the drawbacks and provide even superior tribological performance. However, limited studies exploring the effect of filler combinations on tribological performance under lubricated conditions are available, due to which the following gaps remains in the understanding:

- Limited research exists on which filler combinations perform the best and if material type plays a role, i.e. is having carbonaceous-carbonaceous filler pairs are more effective over carbonaceous- non-carbonaceous filler combinations.
- Although the concept of multi-scale composites has received considerable attention in the recent studies, the focus has predominantly been on combining fillers of varying scales, as a material-variation strategy. Consequently, there is still a limited understanding of whether the observed tribological improvements and the associated mechanisms are primarily due to variations in the material, the scale, or both.
- Little is known about the interaction different fillers may have (filler-filler interaction) and how it affects the tribological performance or if one filler influences the performance of another.
- Additionally, the effect of lubricant on filler performance is not well understood. While a few studies have tested composites performance in different lubricants, it remains unclear how much of the contribution to the tribological performance is due to viscosity effect and what part results from filler-lubricant interactions.

1.8 Hypothesis and Goals

Research hypothesis

- A simultaneous incorporation of a combination of several multiscale carbonaceous and non-carbonaceous reinforcements in a polymer composite can significantly enhance tribological properties of various types of water-lubricated polymers.
- These reinforcements can in addition result in a multifunctional polymer composite properties or their improvements, like mechanical strength, hardness, heat conduction, wetting and others.

- Moreover, selected compositions are expected to have diverse effects in different types of aqueous solutions, which can in some cases result in a notably improved performance in these environments.

Goals and Expected outcomes

- To determine if the selected combinations of multiscale reinforcements can enhance specific or multiple polymer composite properties.
- Explore the effect of load and velocity on the performance of the multiscale polymer composites.
- To determine the effect of different lubricated conditions on the performance of the multiscale polymer composites.
- Examine the change in wear mechanism due to the incorporation of different multi-scale reinforcements.

CHAPTER 2

Materials & Methodology

In Chapter 1, we discussed the introduction, the research problem, and the gaps this work aims to address. Whereas in this chapter, we will explore the materials used, the rationale behind their selection, and the characterisation methods employed.

2.1 Materials used

The materials used included polymer powders; fibrous reinforcements, additives, and particulate fillers incorporated into the polymer to create composites; metal countersurfaces for testing the produced composites; and, lastly, the lubricants.

2.1.1 Polymer powders

Three polymer materials were used as the matrix in this work: UHMWPE, PPS, and PTFE. The selection of these materials was based on the literature review discussed in Chapter 1, section 1.4.2: Tribological performance of neat polymer against metal.

Ultra-high-molecular-weight polyethylene (UHMWPE)

UHMWPE is a thermoplastic polymer characterised by exceptionally long molecular chains (structure shown in Figure 18a), typically exceeding 3.5 million amu in molecular mass. These long chains impart strength and durability, surpassing that of high-density polyethylene (HDPE) and make UHMWPE highly resistant to wear, impact, and various chemicals. UHMWPE is widely used in industries such as food processing, automotive manufacturing, and biomedical applications, particularly for components requiring a long service life and minimal maintenance.

The UHMWPE used in this study was GUR 4170, produced by Celanese (TX, USA) and procured with the help of Resinex (Logatec, Slovenia). The material has an average particle size of 120 μm (d50). This specific grade was selected for its extremely high molecular weight of ~10.3 million amu, the highest available at the time. Since the mechanical properties of the moulded part are expected to be directly proportional to the molecular weight of the polymer, this grade was deemed the most suitable for producing high-strength composites.

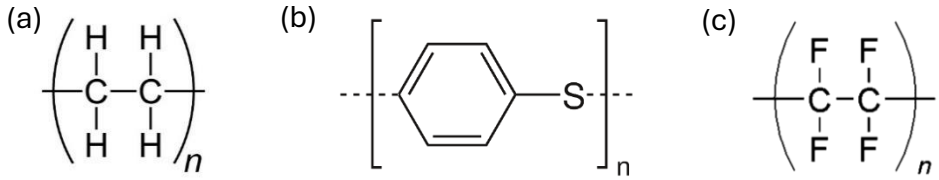

Figure 18 – Chemical structure of polymer matrix used in this study:
(a) UHMWPE, (b) PPS, (c) PTFE

Polyphenylene sulphide (PPS)

PPS is a high-performance, semi-crystalline thermoplastic (structure shown in Figure 18b) known for its exceptional thermal, chemical, and mechanical properties. With a high melting point of around 280°C, PPS retains its strength and rigidity even in extreme conditions, making it ideal for demanding applications. It is highly resistant to chemicals, corrosion, and hydrolysis while also offering excellent dimensional stability and electrical insulation properties. PPS is widely used across industries such as automotive (e.g., engine components, fuel systems), electronics (e.g., connectors, circuit boards), aerospace (e.g., lightweight structural parts), and industrial machinery (e.g., pumps, valves). Its ability to replace metals and thermosets in high-stress environments highlights its versatility and cost-effectiveness.

The PPS used in this study was purchased from Sigma Aldrich (Product No. 182354, CAS No. 25212-74-2). According to the available specifications, it has an average molecular weight of 10,000 amu.

Polytetrafluoroethylene (PTFE)

PTFE, commonly known by the brand name 'Teflon', is a high-performance fluoropolymer (structure shown in Figure 18c) renowned for its exceptional properties. It is chemically inert, offering resistance to nearly all chemicals, and can withstand extreme temperatures ranging from -200°C to 260°C. PTFE has one of the lowest coefficients of friction among solids, making it ideal for non-stick applications such as cookware and low-friction components like bearings and seals. It is also hydrophobic, non-toxic, and highly resistant to UV light, weathering, and electrical currents. These characteristics make PTFE indispensable in chemical processing, automotive, aerospace, electronics, and medical devices.

However, in this work the PTFE was used to blend with PPS. This can abate the brittle behaviour of PPS to some extent as observed in previous studies from the group. The PTFE used for this was also purchased from Sigma Aldrich (Product No. 468096, CAS No. 9002-84-0). The average particle size of the powder is 35 μm based on the provided specification.

2.1.2 Fibrous reinforcements

Based on the literature review, carbon fibres were identified as superior for water-lubricated environments compared to glass and other materials (refer to Chapter 1 Section 1.5.1: Effect of fibrous reinforcements on tribological performance).

In this study, two forms of short carbon fibre were used:

➔ Pristine fibres (100 μm length) – These fibres were produced by Teijin (China) under the product code Tenax HT-M100. These are milled fibres produced without any sizing agent, making it difficult for any material to adhere to them. According to the provided specifications, the powder has a bulk density of 400 g/L.

➔ Recycled fibres (100 μm length) – These are ex-PAN fibres (CF.LS-MLD100) which were obtained from Procotex S.A. corporation (Languidic, France). Since they are recycled fibres, some residual sizing agent is expected to remain on their surface, making it relatively easier for materials to adhere onto them. The carbon content based on available specification is 94 % and bulk density is 350 g/L.

The Raman analysis conducted on both fibres imply the same. As observed in Figure 19, the pristine fibres exhibit only the defect band peak at 1340 cm^{-1} and the graphitic band peak at approximately 1600 cm^{-1}. In contrast, the recycled fibres display additional distinct peaks between 700 and 1250 cm^{-1} and around 2300 cm^{-1}, alongside the defect and graphitic bands.

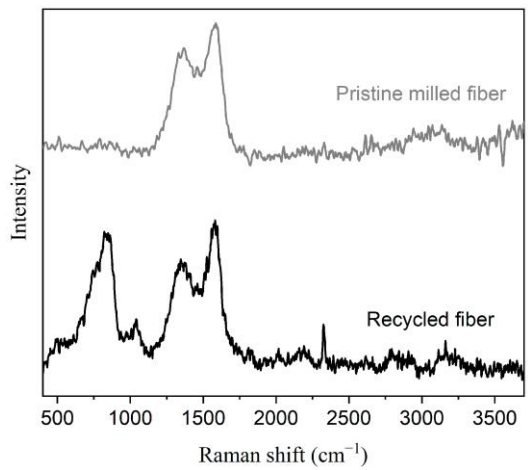

Figure 19 – Raman analysis of the Pristine and Recycled fibres used in this study.

2.1.3 Adhesion improvers and Chain Extenders

As discussed in Chapter 1 Section 1.5.1 & 1.5.2, Compatibilizers might be useful in abating the critical issue of fibre pullout and other challenges observed in previously available studies. Different compatibilizers were used depending on the polymer:

- For UHMWPE, maleic anhydride (MAH)-grafted compatibilizers were used. Two highly reactive MAH with polyethylene as the base chain were selected to help its integration with the matrix. Both compatibilizers were produced and provided by BYK (Wesel, Germany):
  - ➔ SCONA TPPE 1102 PALL – Linear low-density polyethylene (LLDPE)-based
  - ➔ SCONA TPPE 1212 PAHD – High-density polyethylene (HDPE)-based
- Whereas for PPS and PPS/PTFE blend, an epoxy-based compatibilizer, Joncryl ADR 4468, was used. It was produced by BASF (SE, Ludwigshafen, Germany) and supplied by the BTC Chemical Distribution Unit (Copenhagen, Denmark) for this study.

The chemical structure of both compatibilizers is shown in Figure 20.

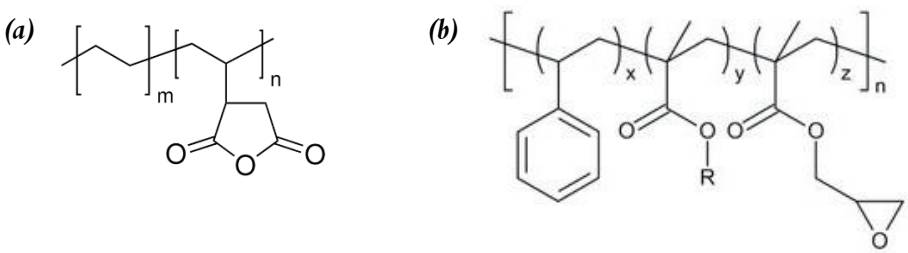

Figure 20 – Chemical structure of compatibilizers (a) MAH grafted polyethylene [108] and (b) Joncryl ADR 4468 [109].

2.1.4 Particulate Fillers

Four particulate fillers were used in this work. Their specifications, based on the datasheets, are provided below. Physical and chemical characterisation of the fillers was also conducted in the laboratory and is detailed in Part II: Appended Papers of this thesis.

- *Graphite* – The graphite used in this work was Timrex KS4, purchased from Imerys (Switzerland). It is a synthetic graphite with particle size of 4.1 μm (d90) and purity

exceeding 99.5 %. Additionally, the selected graphite powder has a very low ash content of 0.07 % and a bulk density of 0.07 gm/cm^3.

- *Hexagonal Boron Nitride (hBN)* – Two grades of hBN were used in this work
  - ➔ The micro boron nitride (Product no. 255475, CAS No. 10043–11–5) was obtained from Merck (USA) in powder form. According to provided specifications, the powder has a purity of 98 %, an average particle size of 1 μm, and a molecular weight of 24.82 gm/mol.
  - ➔ Additionally, a nano-grade of boron nitride (Stock No. NS6130-02-260, CAS No. 10043-11-5) was also used. It was also in powder form produced by Nanoshel (USA), with an average particle size of 60 nm and a purity of 99.8 % according to the specifications.
- *Silicon dioxide (SiO_2)* – The SiO_2 used in this work (Stock No. NS6130-12-000077, CAS No. 7631–86–9) is of hydrophobic nature and was purchased from Nanoshel (UK), also in powder form. Based on its specifications, the powder has a purity of 99.9 %, an average particle size of 1–2 μm and a molecular weight of 60.08 gm/mol.
- *Titanium dioxide (TiO_2)* – A nano grade TiO_2 powder (Product no. 637254, CAS No. 1317–70–0) in anatase form was purchased from Merck (USA). According to provided specifications, the powder has a purity of 99.7 %, an average particle size of 30 nm, and a molecular weight of 79.87 gm/mol.

2.1.5 Lubricants used

Following are the lubricants used in this work

- *Distilled water* was used as the primary lubricant for evaluating the tribological performance all the produced composites. Distilled water lacks bivalent ions such as Ca^{2+}, Mg^{2+}, and Sr^{2+}, which are present in seawater. These ions trigger the formation of carbonates and hydroxides such as $CaCO_3$ and $Mg(OH)_2$ on the metal surface, which are responsible for additional friction reduction, as confirmed with XPS in various studies with sea water [48,110–113]. The absence of these ions in distilled water ensures that any variations in performance can be attributed to incorporated fillers and their reaction products with water.
- *Glycerol* was used as a substitute, whose use was justifiable based on findings from the literature review (refer to Chapter 1, section 1.3: Water and water-based lubricants as an alternative). The glycerol used in this work was purchased from Sigma Aldrich (Product No. 911046, CAS No. 56-81-5). This product is derived entirely from renewable sources, specifically palm tree extract. For tribological testing, a 65:35 mixture of glycerol and distilled water was used. This ratio lowered the freezing point of the mixture below that of water and adjusted its viscosity to

match that of the propylene glycol-based diester (PG, discussed later in the section). Having same viscosity for the two lubricants minimized the effects from lubricant viscosity on tribological performance, thereby the two lubricants (water-glycerol mixture and the diester) could be evenly compared.

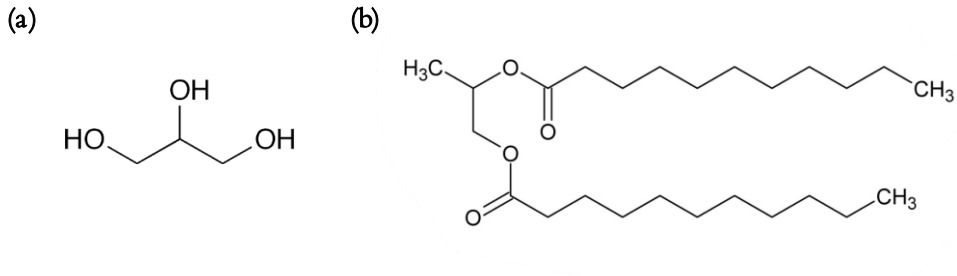

Figure 21 – Chemical structure of (a) Glycerol and (b) Propylene glycol-based ester (PG) [114]

In addition to above, two ester-based lubricants were used for performance comparison and to gain better understanding of the working of other lubricants. Following are the esters used:

- The first synthetic ester is a *propylene glycol-based diester* (termed as PG in this work) which has a vegetable-based fatty acid part. It is produced as RADIA 7208 (CAS No. 68583-51-7) by Oleon (Ertvelde, Belgium) and its structure is shown in Figure 21. Additionally, this ester is termed as 'readily biodegradable' according to the provided OECD 301B rating.

- Another synthetic ester used is commercial ester named *Atlantis 5* (termed as ALT 5 in this work), which is produced by Panolin (Madetswil, Switzerland). It is a saturated synthetic ester with additives for enhancing the corrosion protection and wear resistance. It is also 'readily biodegradable' according to the OECD 301B rating and can be used in marine environment based on the certification from OSPAR commission.

2.1.6 Counter-surface used

The material selected for sliding against produced polymer-composites was *AISI 316 L stainless steel*. It was produced by Inox Center (Nova Gorica, Slovenia) in the form of a 1-meter-long cylindrical rod with a diameter of 40 mm.

From the procured rods, discs with a diameter of 30 mm and a thickness of 5 mm were machined. Subsequently, the surface of the disc was prepared by sequential grinding using different grades of abrasive paper. This was followed by measurements of the surface roughness using Talysurf i-Series pro (Taylor Hobson, UK), a stylus tip profilometer, ensuring a final roughness of 0.10 ± 0.01 μm.

2.2 Preparation of polymer composites

For preparing the polymer-composites, the solvent manufacturing method was used. Ethanol was selected as the solvent, as it was observed to be efficient in segregating all the nano fillers used in this work.

2.2.1 Composite with Particulate Fillers

The process of manufacturing multi-scale composites involves several steps, each explained in step-by-step manner below.

a. Segregation of Particulate Fillers

To disperse the fillers, probe sonication was used. The ultrasonic power supply generates high-frequency electrical signals, which are converted into mechanical vibrations. These longitudinal vibrations are amplified by the probe and transmitted into the liquid, creating pressure fluctuations that generate shock waves (extreme in pressure and temperature) capable of disrupting nano-particle agglomeration.

To ensure that deagglomerated nano-particles do not attach with micro-particles, the batch was kept separate based on their scale as shown in Figure 22. Initially, only fillers are sonicated with around 20 mL of solvent. In the case of nano-particles, the sonication time depended on the dynamic light scattering (DLS) analysis conducted on the filler. Meanwhile for micro-particles, it was fixed at 30 minutes. Following this, a portion of polymer powder was added to each dispersion (or entire polymer to it in case creating a micro-composite) and the mixture was sonicated again to ensure the dispersed fillers adhere to the polymer. Finally, the batch containing micro fillers was added to the nano filler batch and given an additional sonication cycle. This final sonication step was skipped when creating a micro-composite.

b. Ball milling

The entire mixture then goes through extensive homogenization on a planetary ball mill. This was done by placing the slurry mixture from the previous step into a cup with zirconia balls, so that the weight of the mixture to that of accumulated weight of zirconia balls was 1:5. The milling process was carried out for 2 hours at 200 rpm. The equipment used for this was PM 100 planetary ball mill manufactured by Retsch GmbH (Haan, Germany).

c. Drying

After ball milling, the homogenised mixture was separated from the zirconia balls and left to dry for 24 hours. In case of UHMWPE composites, the temperature is set to 65 °C while drying, while for PPS higher temperature of 75 °C is used.

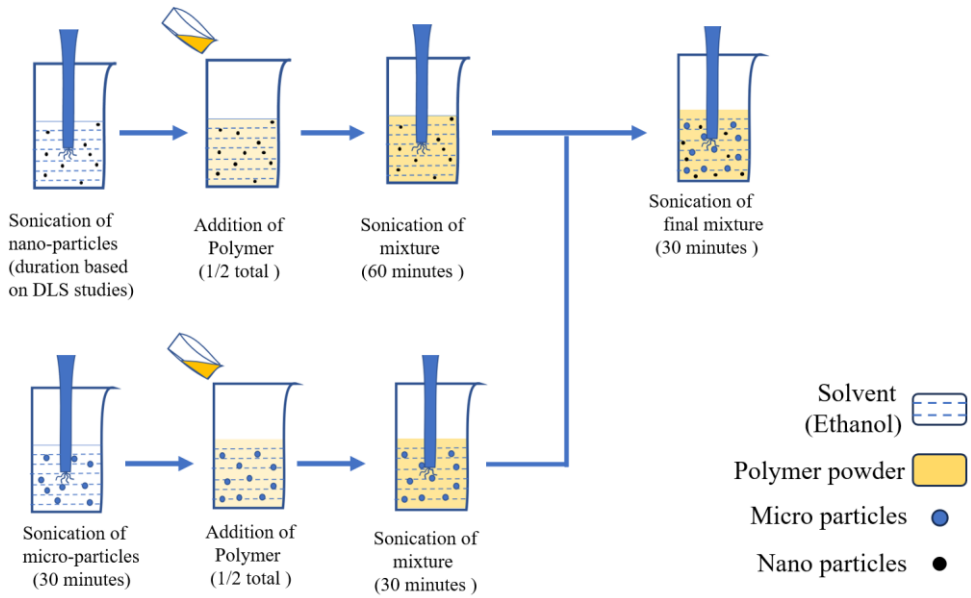

Figure 22 – Process used for segregation of particulate fillers for creating multiscale composites.

d. Short milling with fibres

Once the solvent is evaporated during drying process, a dry homogenised powder remains behind. This powder then undergoes another round of ball milling, though less extensive compared to previous stage. In this stage, the dried powder is added with set quantity of short carbon fibres and zirconia balls. The ratio of mixture to ball is kept at only 1:2 and the milling duration is just 5 minutes at 100 rpm to minimize fibre breakage that might occur from milling.

e. Moulding

Before moulding the powder was re-dried for 24 hours to ensure there was no moisture or solvent remaining in it. Following this step, the procedure differed depending on the polymer material.

➔ For UHMWPE composites, Compression moulding was used for preparing the composites. The equipment used for this purpose was LZT-UK-35-L Laboratory press by Langzauner GmbH (Lambrechten, Austria). The entire process is illustrated in step form in Figure 23.

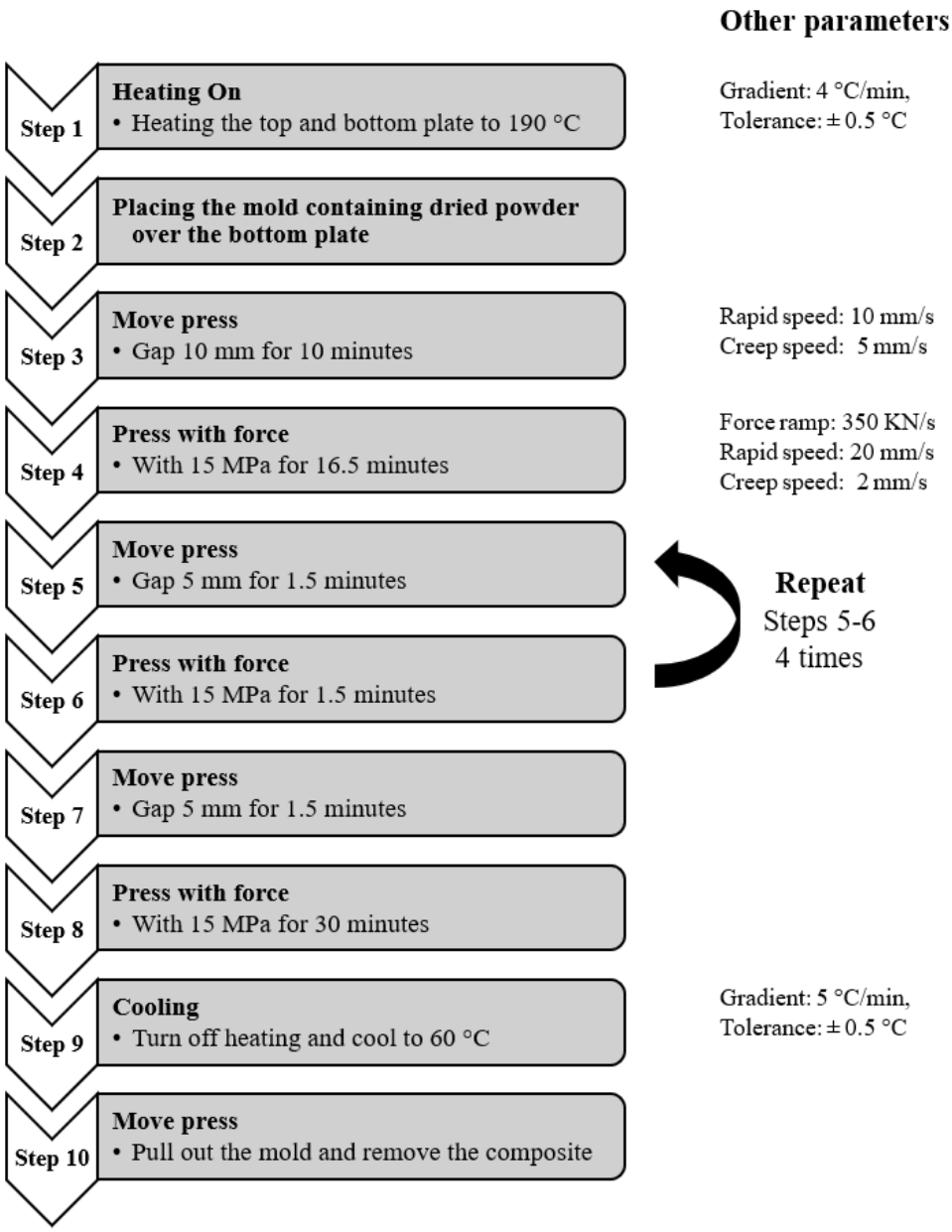

Figure 23 – Process used for compression moulding for preparing UHMWPE composites.

➔ For PPS and PPS/PTFE blends on the other hand, injection moulding was employed for preparing the composites. This was done using a Hakke Minijet pro piston injection moulding machine manufactured by Thermo Fisher (Karlsruhe, Germany). The dried powder mixture was loaded into the cylinder and parameters listed in Table 4 were used to make the composites.

Table 4: Parameters used for injection moulding

	Parameter	Value
Pressure	Pressing	500 bars
	Post Pressing	300 bars
Temperature	Cylinder	315 or 375 °C
	Mold	200 °C
Time	Injection	45 sec
	Hold	15 sec

2.2.2 Incorporation of compatibilizers

For all selected compatibilizers, two locations in the manufacturing process discussed in sub-section 2.2.1 were chosen. The first incorporation location was with the polymer in step a. (Segregation of Particulate Fillers) and the second location was prior to step e. (moulding).

2.3 Performance evaluation

2.3.1 Thermal characterization of composite material

Differential scanning calorimetry (DSC) was used to examine the changes in the melting peaks and crystallinity of the polymers in the presence of fillers. Crystallinity of the polymer is an important property, as it indicates the composite's susceptibility to water absorption. When polymers are exposed to an aqueous environment, water molecules can more easily penetrate the amorphous regions, thereby altering properties such as strength, hardness, and contact angle [106,115,116]. In contrast, the crystallites are impenetrable for non-reactive molecules [117,118]. Since crystallinity indicates the percentage of crystallites/non-amorphous zones, a higher crystallinity for the polymer indicates lower water absorption from it.

The measurements were made using a DSC-2 instrument by Mettler Toledo (USA). Samples of composite material weighing 10 mg were placed in standard alumina crucibles and heated in a nitrogen environment at a flow rate of 80 mL/min for all the measurements. The samples were initially heated to 200 °C and

kept there for 5 min to erase residual stresses and minimize other effects that derived from manufacturing. After this the samples were cooled to 25 °C and subjected to a second heating cycle. The heating and cooling rates were maintained at a constant 10 °C/min. The crystallinity (X_c) was determined based on the average of two measurements. For both heating cycles, the crystallinity was calculated using the following equation:

$$X_c = \frac{\Delta H}{(100 - \text{fc}).\times \Delta H_{100}} \times 100$$

where fc is the fraction of filler concentration in the composite material, ΔH is the enthalpy of fusion determined using the melting peak and ΔH_{100} is the enthalpy of fusion for 100 % crystalline polymer.

2.3.2 Surface characterization of composite material

Wettability

The composite's affinity towards water is expected to influence its tribological performance. A more hydrophobic composite, when tested with water as a lubricant, will have lower water absorption. To determine the affinity of polymer-composites towards water, contact-angle measurements were performed on the surface of the composite using an optical goniometer, the CAM101 tensiometer by KSV Instruments (Finland). Drops of distilled water with volume of approximately 4 μL were carefully placed on the surface of interest, and the contact angles were measured. A total of 10 measurements were made along the surface for each composition.

2.3.3 Mechanical characterization of composite material

Hardness

The hardness of the polymer-composites was determined using Vickers method. Measurements were carried out on a Duramin AC40 instrument manufactured by Struers (Denmark) with a diamond cone as the indenter. A total of 10 measurements were made, each with a dwell time of 10 s. The loading used varied depending on the polymer material. The resulting hardness values (HV) were determined as follows:

$$\text{HV} = k \times \frac{\text{P}}{d^2} \times 10^6$$

where 'd′ is the average diagonal length of the indentation, 'P′ is the load, and 'k′ is a geometrical factor.

Impact strength

The Impact strength measurements were conducted according to the standard for impact properties of plastics (ISO 179). The samples had dimensions of 80 × 10 × 4 mm^3. Three tests were performed for the average value and variation in the impact strength.

Density

The density of composites was measured according to ASTM D 792-86 (displacement) method using an electronic balance as per the following equation

$$\rho = \rho_{Liquid} \cdot \frac{W_{air}}{(W_{air} - W_{Liquid})}$$

where ρ is density of the sample, ρ_{Liquid} is the density of liquid used, W_{air} is the weight of the sample in air and W_{Liquid} is the weight of the volume of liquid displaced when the sample is fully immersed into the liquid.

2.3.4 Tribological characterization of composite material against 316L steel.

Testing of the produced composites was carried out in reciprocating mode using a pin-on-disk arrangement on a Cameron Plint TE-77 tribometer produced by Phoenix Tribology (UK). The equipment is shown in Figure 24. The arrangement consisted of a steel disk that was fully submerged in the lubricant and a polymer-composite pin sliding on top of it. Additionally, the equipment also has a heating plate beneath the lubricant container to maintain the lubricant at a specific temperature throughout the test if required.

All the composites produced were tested at two loads corresponding to a contact pressure of 5 and 15 MPa. The other test parameters were 0.1 m/s for the relative velocity and 10.6 mm for the stroke length, which were kept the same for all the tests performed. Each test ran for 20 hours, i.e., a total sliding distance of 7200 m.

Additionally, start stop tests were performed for specific composite and lubricant combinations. For these tests, after running for 20 hours, the test was stopped and the contact disengaged for 4 hours. The test was then restarted, but with a different load and velocity. The cycle of stopping, disengaging and restarting the test with different load and speed was then continued.

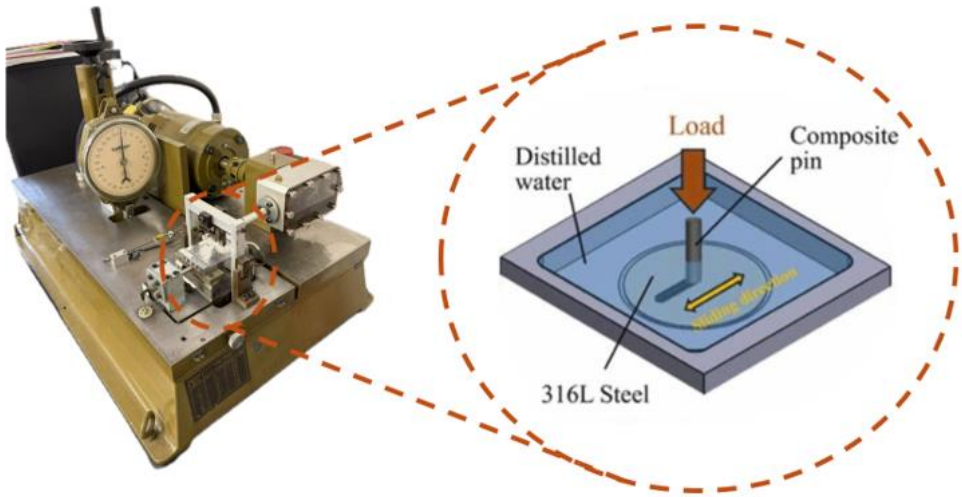

Figure 24 – Equipment on which the tribological tests were performed (left) and schematic showing the arrangement of components (right)

Calculation of steady-state coefficient of friction and wear rate

During the final 8 hours, the friction was stabilized in all the tests and the average was used as the steady-state coefficient of friction. Wear was determined in terms of wear volume using the calculated density for the compositions and the change in weight of the pins before and after the test. Even though water absorption by the UHMWPE composites was expected to be negligible during the 20-hour test period [45], the pins were dried in an oven for 48 h at 65 °C to ensure the drying out of any remaining water. The wear volume (wv) and specific wear rate (k0) were calculated as:

$$w_v = \frac{\Delta w}{\rho} \ (mm^3)$$

$$k_0 = \frac{\Delta w}{\rho \,.\, P \,.\, L} \ (mm^3 / N \,.\, m)$$

where Δw is the weight difference before and after the tests (mg), ρ is the density of the composite material (mg/mm^3), P is the normal load (N), and L is the sliding distance (m).

While the water absorption by UHMWPE composites was known to be minuscule, absorption of other lubricants could vary, thereby when comparing wear rate in different lubricants, the wear rate was calculated using change in length of the polymer-composite pin as

$$k_0 = \frac{\Delta l \,.\, \pi \,.\, r^2}{P \,.\, L} \quad (mm^3 / N \,.\, m)$$

where Δl is the length change before and after the tests (mm), r is the radius of the composite pin (mm), P is the normal load (N), and L is the sliding distance (m).

Finally, to ensure repeatability, three tests were made for each condition and the average values, as well as the standard deviations, of the coefficient of friction, wear volume and specific wear rate were recorded.

2.3.5 Post characterization of worn surfaces from tribological tests

Physical characterization

Scanning electron microscopy (SEM)

To determine the wear mechanisms, the worn surfaces of the polymer-composite and steel were observed under a scanning electron microscope. The instrument used for this was JSM IT100 manufactured by JEOL (Japan). Due to the non-conductive nature of the polymer material, the composite pins were gold sputtered prior to the observation (SCD005, Baltec AG, Liechtenstein) with a coating thickness of approximately 12 nm (sputtered at a 50-mm working distance using 30 mA for 80 s). This step was not required when observing the steel discs for a transfer film, as only a very small amount of charge accumulation was noticed when acquiring images from the wear tracks. The acceleration voltage used for the secondary-electron (SE) images was 10 kV.

Atomic force microscopy (AFM)

The wear tracks on the steel surface were also examined using an atomic force microscope to analyse the changes in the topography and inspect the state of any additional material present over the steel surface. The equipment used for this was MFP-3D Origin manufactured by Asylum Research (UK). Scans inside the wear-track region were performed for all the compositions and test conditions. The scans covered an area of 30 × 30 μm^2 at a speed of 0.15 Hz in continuous-contact mode. The tip used was an AC240TS-R3, which has a spring constant of approximately 2 N/m, and is therefore also suitable for mapping the topography of softer materials that might have adhered to the steel surface during sliding. The generated topography data were analysed and processed using Gwyddion software (version 2.65).

Lateral force microscopy (LFM)

In addition to AFM, lateral force microscopy was performed inside the wear-track region on the steel disks of selective compositions. This analysis aimed to provide insight into the role of the material present over the steel surface in the observed friction

behaviour. For this, the AFM tip was first allowed to slide over the material covering the steel surface for an extended period so that the material could adhere to the tip (Raman spectroscopy was used to conform the presence of adhered material over the tip). Following this, the tip with adhered material was made to slide over a new area on the steel disc wear track and the lateral voltage, thereby the lateral force was evaluated. Since the tip already bore the same transfer material from the polymer-composite as the one covering the steel disc, the system effectively simulated a transfer material-to-transfer material sliding interface.

White light interferometry

The worn surfaces of the polymer-composite were also examined using an optical interferometer for evaluating the condition of the carbon fibres after sliding. The equipment used for this was Contour GT-K0 produced by Bruker (USA). The analysis was done in a high-resolution vertical scanning interferometry (VSI) mode with a 50 × objective and a white-light source. The data were analysed and processed using the onboard Vision 64 software.

Nano Indentation

The wear-track region on the steel surface was analysed using a nano indenter (Step 700 + UNHT^3, Anton Paar, Austria) to determine the thickness and hardness of the material transferred from the composite. This was conducted using a Berkovich (BS-47) pyramid-shaped diamond indenter in sinusoidal loading mode, which allowed for an evaluation of the hardness along the indentation depth. The main curve employed a constant strain-rate loading from 0 to 95 mN, with the loading rate/load being set to 0.05 1/s and a 30-second pause upon reaching the maximum load. The contact force was set to 0.3 mN for the main curve. The additional sinusoidal loading alongside the main curve had an amplitude of 5 mN and a frequency of 5 Hz. To validate the results and observe the variation with location on the surface, 6 indents were made, placed at a distance of 50 micrometres in form of a 2 × 3 matrix on each sample. The harness of the transferred material was determined using the following

$$H_f = \frac{(1 - h_f/h_t)^2 . H_s - H_c}{(1 - h_f/h_t)^2 - 1}$$

where H_f is the hardness of the transferred material layer over the steel surface (GPa), H_s is the hardness of the underlying steel (GPa), H_c is the combined hardness from the transferred material layer and steel evaluated from the main curve (GPa), h_f is the thickness of the transferred material layer evaluated using the sinusoidal curve (nm) and h_t is the total penetration depth of the indenter (nm).

Chemical characterization

Energy dispersive X-ray (EDS) analysis

To assess the distribution of these elements in the analysed areas, elemental maps were also produced in addition to SEM. The acceleration voltage used for EDS was 20 kV.

Raman spectroscopy

The wear tracks on the steel surfaces were also examined using Raman spectroscopy to determine the formation of the transfer layer and the adhesion of constituents during sliding. The equipment used for this was Scientific XploRA Plus V1.2 Raman spectrometer produced by Horiba (Japan). Spectra were taken from wear tracks on the steel disc for the range 300 to 4000 cm^{-1}. The laser used for this purpose had wavelengths of 532 (with the filter set to 25 %) and 638 nm (with the filter set to 50 %), which was selected after confirming their interaction with the polymers and all the fillers used in the composition. To keep the analysis limited to the transfer layer, a 50 × objective was used. This kept the vertical resolution confined to about 2 μm. Other parameters included the selection of the grating (1200 nm), the hole (300 μm), and the slit size (100 μm).

X-ray photoelectron spectroscopy

To track the chemical interactions that occurred during the tribological testing, both the surface of the composite pin and the wear tracks were analyzed using X-ray photoelectron spectroscopy (XPS). These analyses were performed on a PHI TFA XPS spectrometer produced by Physical Electronics (USA) using an Al Kα monochromatic source for the irradiation. Region of 400 μm in diameter on the surface was excited with X-rays and the emitted photoelectrons were collected originating typically from a depth of 3–5 nm. The composition of the worn pin's surface was determined from the peaks corresponding to C 1 s, B 1 s, O 1 s, N 1 s, considering the relative sensitivity factors provided by the manufacturer. Due to possible charging of the surface, the C 1 s spectra were shifted to 284.8 eV prior to the deconvolution. For quantifying the composition on the steel surface, C 1 s, N 1 s, O 1 s and Fe 2p peaks were used. Further, for analyzing the changes occurring underneath the surface of the pin and the steel, ion etching was performed using an Ar-ion beam of energy 1 keV for different etching times. The estimated etching rate was 1 nm/min.

2.3.6 Lubricant analysis

For selective cases, the lubricant obtained from the tribological tests was also analysed using Raman and Fourier Transform Infrared (FTIR) Spectroscopy to detect any variations compared to original.

CHAPTER 3

Results and Discussion

Following the literature review in Chapter 1, which identified gaps leading to the research problems, and the methodology outlined in Chapter 2, this chapter presents the results of the work. The findings are presented step-by-step, reflecting the four publications derived from this work. Alongside the outcomes of each publication, a 'Conclusion and Next steps' section is provided highlighting the major takeaways and the reasoning behind subsequent publication.

The first step involved mitigating the known issues with the selected materials, namely fibre pullout and brittle behaviour of selective polymer materials. As outlined earlier, compatibilizers (refer sub-section 2.1.3: Adhesion improvers and Chain Extenders) were introduced into the polymers (refer sub-section 2.1.1: Polymer powders) and filler systems (refer sub-section 2.1.2: Fibrous reinforcements) using the manufacturing process described in sub-section 2.2.2: Incorporation of compatibilizers. Below are briefly summarised the results and mechanisms as part of Paper A.

3.1 Paper A

Title - Does a Compatibilizer Enhance the Properties of Carbon Fiber-Reinforced Composites ?

Outcomes from the publication

The incorporation of compatibilizers affected properties like hardness, impact strength, wettability and crystallinity. These effects depended on the polymer type, compatibilizer incorporation location, and manufacturing temperature.

For UHMWPE, the introduction of the compatibilizer showed a decline in material's impact strength. This reduction was more pronounced when the compatibilizer was added before the moulding stage. The material's hardness on the other hand had no effect from compatibilizer. Comparison of compatibilizer types revealed only a marginal difference, with the HDPE-based option performing slightly better than the LLDPE-based one. Lastly, the addition of the compatibilizer did not affect the material's wettability or the polymer's crystallinity.

For PPS-based compositions, the compatibilizer could only be incorporated before the moulding stage due to its low glass transition temperature. Having 1.5 wt. % of compatibilizer in presence of either SCF or PTFE improved hardness by 10-13 % and impact strength by up to 20 %. However, when both SCF and PTFE were present, a higher concentration of compatibilizer (about 3 wt. %) was required to match above improvements. A variation in crystallinity of polymer materials was also noted with compatibilizer. A decrease was observed for PPS by around 7 %. In contrast, an increase in crystallinity for PTFE by 4-5 % was noted. The manufacturing temperature had negligible effect in the absence of PTFE. With PTFE present, hardness and impact strength values were 10 % greater with higher cylinder temperatures (375 °C). Additionally, the material's wettability varied significantly with manufacturing temperature capable of increasing or decreasing the contact angle by up to 10°.

To understand the mechanisms, several analyses were carried out on selected samples:

- The FTIR analysis carried on UHMWPE powders and compositions revealed that chosen compatibilizers lose their polarity in the presence of the solvent, rendering them unsuitable for introduction before or during the manufacturing process.
- Meanwhile, the micrography of the fractured UHMWPE composites from impact testing implied that when the compatibilizer was added before moulding, it remained agglomerated and possibly acted as stress concentration sites.
- The SEM and EDS analysis on PPS based compositions, showed improvement in homogeneity between different components and fibre-polymer interface when the compatibilizers were present, supporting the observed variation in hardness and strength.
- The FTIR analysis conducted on PPS based compositions demonstrated that the compatibilizer was consumed, as indicated by a diminished C–O–C linkage after moulding. One way PPS chains end is with a –Cl group, the reduction in area under C-Cl peak with the introduction of compatibilizer in association with reduced crystallinity indicate chain extension, whereas peaks in N–H region points to possible bonding with groups on fibres. Further, the variation in CF_2 and CF_3 peaks aligned with the observed wettability results.

Conclusion and Next steps

The improvement observed with compatibilizers make PPS-based composites more useful in already-established applications (such as gears or bearings) where resistance to impact loading and durability are essential. Additionally, the ability to adjust the material's wettability by changing the manufacturing temperature in the presence of compatibilizers further expands their potential use in components such as pumps and valves.

However, the highest values recorded for hardness and impact strength upon incorporation of compatibilizer into PPS/PTFE blend with SCF as reinforcement were 27 H.V0.5 and 17.5 KJ/m^2 respectively. Which even though is a huge improvement compared to neat PPS, still insignificant compared to UHMWPE which stands at 100 KJ/m^2 without any reinforcements. Additionally, compatibilizers increased the melt viscosity, which would likely rise further with introduction of particulate fillers in the composition. This limited the concentration of fillers that could be incorporate in the PPS based composites.

This led to a choice between the following two approaches for future work:

- *Reduced filler concentration in PPS composites* and rely on compatibilizers for issues such as brittle material behaviour and fibre-polymer interface.
- Use *optimum concentration of fillers* (based on literature) *using UHMWPE as the polymer matrix*.

After careful consideration, the latter option was selected. Thereby, UHWMPE was selected as the base polymer material for subsequent publications to address the research questions outlined in sub-section 1.8. Since, compatibilizers did not work for UHMWPE in our selected manufacturing process, incorporating another filler to deal with the known issues of fibre pullout with the material was tried.

3.2 Paper B

Title - Effect of multi-scale fillers on the tribological behavior of UHMWPE composites in water-lubricated contacts

This study addresses research gaps and hypotheses related to how simultaneous incorporation of several carbonaceous and non-carbonaceous fillers into the polymer affects composite properties such as hardness, crystallinity of polymer, wettability and tribological performance of the composite material against steel under distilled water-lubricated conditions. Moreover, emphasis was placed on understanding the role of filler scale in these properties, to determine whether improvements stem from the filler material itself or its size. This helps clarify whether developing multi-scale composites is justified.

For this, three fillers were incorporated into the UHMWPE polymer, namely SCF, graphite and hexagonal boron nitride (h-BN). To test whether carbonaceous-carbonaceous filler pairs (e.g., SCF-graphite) perform better than carbonaceous-non-carbonaceous pairs (e.g., SCF-hBN), compositions with 10 wt.% micro-scale fillers were prepared. Additionally, a composition with all three fillers was also prepared. Further, to analyse the effect of filler scale, multi-scale compositions containing same

concentration of fillers as the micro-scale compositions were prepared by replacing 3 wt.% of micro-hBN in the composition with equal wt. % of nano-hBN.

Outcomes from the publication

The results indicated varying effects on composite's properties from having several fillers and their scale. For example, the hardness of the composite improved with the inclusion of several fillers. Selective combination of fillers showed a higher hardness value compared to other combinations (for instance, composite with SCF and Graphite showed higher hardness value than one with SCF and h-BN), implying filler material played a role for the property. However, the highest hardness was recorded in a composition containing all the selected fillers, suggesting a cumulative effect and incorporation of several fillers to be beneficial. Additionally, the scale of the fillers played a role, as multi-scale composites demonstrated hardness value 10 % greater than a micro-scale composite with the same filler concentration.

Not all properties displayed this cumulative effect. In the case of wettability, SCF was the dominant filler in determining the contact angle. The addition of other fillers, combinations of fillers, or the scale only demonstrated marginal changes (less than 4°), which is within the range of measurement error.

Furthermore, the inclusion of fillers did not always yield a positive impact; some properties deteriorated with specific fillers. For example, the crystallinity of the polymer was reduced by the presence of carbon-based fillers, such as SCF and Graphite. This reduction was more severe when both carbon-based fillers were used together, with crystallinity levels up to 15% lower than those of UHMWPE without fillers. However, adding h-BN helped to abate this deterioration, suggesting presence of several fillers to be beneficial. The filler scale, on the other hand, had no effect on crystallinity.

The tribological performance of the composite containing all the selected fillers was found to be the best. This micro composite was able to sustain much higher loads (corresponding to 15 MPa) than pure UHMWPE, had friction performance comparable to that of other composition with graphite (coefficient of friction ranging between 0.065 and 0.085) and wear rate similar to those composition with h-BN (ranging between 1 and 3 x 10E-7 $mm^3/N.m$). Moreover, the filler scale played a role, as the multi-scale composite showed up to a 40% lower coefficient of friction (ranging between 0.05 and 0.06) compared to a similar micro composite with the same filler concentration.

The analysis of the worn surfaces provided significant insights into the role of different fillers and possible filler interactions in the observed performance:

- The SEM analysis demonstrated that composites containing only carbon-based fillers exhibited fibre pullout. In contrast, those with h-BN did not show this sign. The EDS and XPS analyses indicated that diboron trioxide formed during sliding and accumulated at cracks or the fibre–polymer interface, which helped to prevent fibre pullout as shown in Figure 25a.

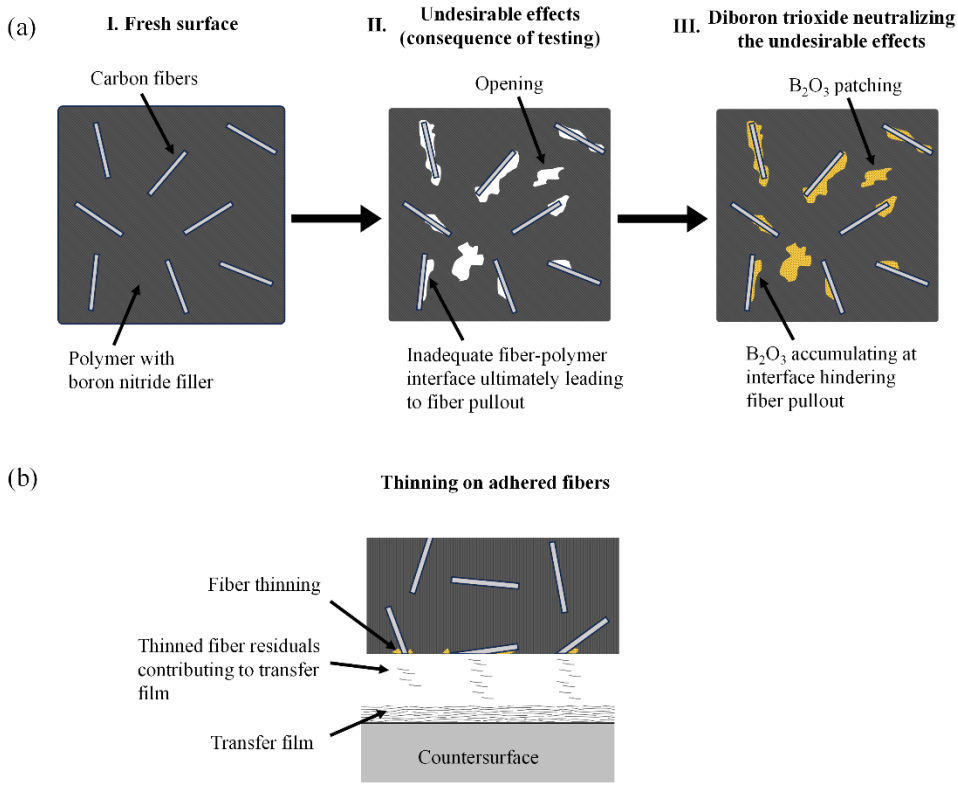

Figure 25 – Proposed mechanism showing (a) test causing the fresh composite surface (I) to develop undesirable features (II) and accumulation of B_2O_3 impeding the worsening of these features (III), (b) side view illustrating fiber thinning taking place at the composite pin and residuals contributing to the transfer film on the steel disc. Valid for compositions containing boron nitride.

- The SEM analysis of steel discs on the other hand, revealed material adhering to the surface in wear track region. The Raman and XPS analysis of the adhered material identified it to be carbon-based (specifically SCF and Graphite), suggesting a strong affinity between carbonaceous materials and metals. In many cases, no fibres were found on the worn surface, suggesting the material over steel surface to be from

residual from fibre thinning, which was also confirmed by AFM analysis of the composite surfaces.

- The Raman spectra from the wear tracks on the steel disc showed that the I_D/I_G ratio was lower for the multi-scale composition compared to the micro-composition. This suggests a higher graphitic-like crystalline structure in the transfer film of the nano-composition. Additionally, the XPS analysis also indicated an increased concentration of C-OH bonds for the multi-scale composition.

  Note: An increase in H-H, H-OH, and OH-OH groups also support lower coefficient of friction due to repulsive actions between these bonds. Additionally, with more comprehensive thinning occurring on the composite pin, a higher concentration of residual material is expected to transfer onto the steel disc.

- The Raman and XPS analysis of the steel disc wear track indicated no transfer of boron related materials from the polymer composite. Additionally, the Raman and FTIR analysis of the lubricant obtained from tribological tests implied that any boron-related material present was below the measurable concentration.

Conclusion and Next steps

The results demonstrate that incorporating several fillers into the polymer-composites let to improved properties such as hardness and tribological performance. Additionally, combining carbonaceous and non-carbonaceous fillers helped abate the loss of polymer crystallinity.

The composite containing several fillers type had the lowest wear volume and coefficient of friction, indicating synergistic behaviour between the fillers irrespective of the scale. Further it was observed that having h-BN caused SCF to contribute to the tribological performance, implying positive outcome from filler interaction.

Additionally, it was observed that Nano fillers, owing to their higher surface area and superior interfacial interaction with the matrix material, exhibit a more uniform dispersion within the polymer material and around the carbon fibres compared to micro fillers in the composite. As a result, entire fibres or portions of partially thinned fibres being pulled from the composite pin into the transfer material on the steel surface, due to the absence of hBN around them, is less likely to happen in multi-scale composition. This could account for the higher graphitic content in the transfer film for compositions with nano-fillers, as more comprehensive thinning is anticipated before pullout occurs. This is why the multi-scale composition had a more coherent film with better coverage, overall leading to a much lower coefficient of friction in tribotesting. Overall, both filler type and scale had effect on the tribological performance observed from the composite.

As observed from the literature review that the working of hard and soft particulate fillers can vary significantly (see section 1.5.3: Fillers for improving tribo-performance). Since the particulate fillers used in this study were soft and less is known how filler interaction will vary if one of the selected fillers is hard. Therefore, to better understand the above, similar study with hard filler is needed, which is the basis for next study, denoted as Paper C.

3.3 Paper C

Title - Tribological behaviour of nano-titanium dioxide filled UHMWPE composites with a variety of micro fillers based on carbon, boron nitride and silicon dioxide under water-lubricated condition

Hard inorganic fillers, such as aluminium oxide and zirconium oxide, are also expected to contribute to the transferred material, thereby improving the tribological performance through surface separation and acting as rolling elements because of their spherical shape. However, limited knowledge is available on the tribological performance and working mechanism of these hard inorganic fillers in combination with other fillers, especially under water-lubricated conditions.

In this study we combine nano-scale titanium dioxide with other fillers whose working mechanisms when in combination are well researched. This is to see how the interaction between the fillers varies upon having hard filler into the composition. The polymer matrix used for this is UHMWPE and the other fillers used in combination are graphite, hexagonal boron nitride (h-BN) and silicon dioxide, all of the same scale. Moreover, as it was observed in the previous study that for UHMWPE to be able to bear high loads, fibrous reinforcements were necessary. Therefore, all prepared compositions were reinforced with SCF. Further, the compositions prepared for this had titanium dioxide in nano scale, always in same concentration of 5 wt.% and one of the above micro scale fillers in 10 wt.% concentration.

Outcomes from the publication

The results indicated varying effects in composite properties upon combining titanium dioxide with various carbonaceous and non-carbonaceous fillers.

The hardness of the composite was observed to increase with the incorporation of additional filler in the titanium dioxide-containing fibre-reinforced UHMWPE composite. With the inclusion of graphite as the additional filler in the titanium dioxide and SCF-containing composition, a hardness of 8.03 H.V. was noted, which was 53 % higher compared to the same composition lacking graphite. With h-BN or silicon dioxide as additional filler, on the other hand, the increase in hardness was only about

15 % compared to titanium dioxide-containing fibre-reinforced UHMWPE composite without these additional fillers.

Not all properties showed variation with the inclusion of additional filler to the titanium dioxide-containing fibre-reinforced UHMWPE composition. For example, the crystallinity of the polymer in the produced composites was noted to range between 47–51 %, irrespective of the inclusion of additional filler into the titanium dioxide composition or the material of the additional filler. The above variation is within the margin of error for the measurements.

Surface wettability, on the other hand, showed variation in either direction with the inclusion of additional filler to the titanium dioxide and SCF-containing composition. With the inclusion of graphite or h-BN as the additional filler, the contact angle showed a slight reduction of 2–3 degrees, which is marginal. Whereas with silicon dioxide as an additional filler, an increase of 8 degrees in contact angle was noted compared to the titanium dioxide-containing fibre-reinforced UHMWPE composite lacking the additional filler. The highest contact angle noted was with the inclusion of silicon dioxide as the additional filler, having a value of 108 degrees.

Overall, no significant detrimental effects were observed in composite properties with the inclusion of additional filler in the fibre-reinforced titanium dioxide composition.

The effect of having additional filler on the tribological performance of the produced titanium dioxide composites was noted to be dependent on the filler material and the contact pressure. At a low contact pressure of 5 MPa, the results implied having any of the additional fillers (graphite, h-BN or silicon dioxide) had no effect on the friction performance of the composite-steel pair, as the coefficient of friction was noted to be about 0.08 for all compositions. In contrast, the wear results at 5 MPa showed a reduction in wear rate for the titanium dioxide compositions with the incorporation of additional filler. Additionally, the wear rate was noted to be dependent on the additional filler material. The lowest wear rate was noted with graphite as the additional filler, exhibiting a value of 8.2×10^{-8} mm³/N, which is an 86% reduction compared to the titanium dioxide-containing fibre-reinforced UHMWPE composite lacking any additional filler. Meanwhile, the reduction noted with h-BN and silicon dioxide as additional fillers was 83% and 53% respectively.

At a higher contact pressure of 15 MPa, the results implied selective fillers to be contributing to the frictional performance. For compositions with h-BN and silicon dioxide as fillers, the coefficient of friction was about 0.05, which is about 32% lower compared to the fibre-reinforced titanium dioxide composition lacking these additional fillers. Meanwhile, for the composition with graphite as the additional filler, the coefficient of friction was again noted to be similar to the fibre-reinforced titanium dioxide composition, i.e. between 0.075–0.080. The wear rate at 15 MPa, on the other

hand, followed the same trend as observed at 5 MPa, where the lowest wear was noted with graphite as the additional filler, followed by h-BN and silicon dioxide.

The analysis of the worn surfaces provided significant insights into the role of different fillers and possible filler interactions in the observed performance:

- The SEM analysis of the worn polymer-composite surface demonstrated that the composite containing only SCF and titanium dioxide as fillers exhibited fibre pullout. In contrast, composites with graphite and h-BN as additional fillers did not show this sign. Meanwhile, the composite with silicon dioxide as an additional filler still exhibited signs of fibre pullout.

- The optical interferometry of the worn polymer-composite revealed the adhered fibres in most cases to have a flatter profile compared to fresh fibres, implying fibre thinning taking place during sliding.

- The SEM analysis of steel discs, on the other hand, revealed material adhered to the surface in the wear track region, with coverage varying between compositions. The highest coverage was noted for wear tracks from compositions containing h-BN as the additional filler, whereas the lowest coverage was noted for the wear track from the fibre-reinforced titanium dioxide composition lacking any additional fillers.

- The Raman analysis of the material adhered onto the steel disc revealed D-G bands for all compositions, implying the residue from fibre thinning contributed to the adhered material. For the composition with graphite as the additional filler, an extra apex for the G-band was noted, implying graphite contributed to the transferred material as well. Additionally, the results from spectroscopy implied presence of titanium dioxide in the adhered material for selective compositions, and only in wear tracks obtained from testing at high pressure.

- The transfer of graphite and titanium dioxide to the steel surface in the wear track region was confirmed with AFM and nano-indentation. The nano-indentation showed the transferred material over the steel disc wear track to have lower hardness for the composition with graphite, and significantly higher hardness for wear tracks where Raman spectroscopy indicated the presence of titanium dioxide. The AFM indicated materials matching the dimensions of used graphite and titanium dioxide to be present in the wear track region. However, the graphite was noted to have a lower lateral dimension, and titanium dioxide nanoparticles were noted to be embedded in the surrounding transferred material.

- The results of lateral force microscopy conducted over the material adhered onto the steel disc showed significantly lower lateral force in cases where titanium dioxide was present in the adhered material.

Conclusion and Next steps

Based on the results, it was observed that the selected hard filler (titanium dioxide) contributed to the tribological performance even in the presence of all the other fillers in the composition. Further, the friction behaviour of the polymer composite–steel pair depended on factors including the composition of the material transferred to the steel surface, its coverage, and its ability to cover the rough surface of the steel. The wear of the composite, however, mainly depended on the fibres' ability to remain adhered, in which other fillers played a dominant role.

Upon combining with only carbon-based filler in the composite, the nano-titanium dioxide was absent from the material transferred to the steel surface, and a higher friction was observed. However, with other non-carbon-based fillers present in the composition, the nano-titanium dioxide was part of the transferred material, where it was found embedded in a relatively softer layer of material composed of other components transferred from the composite.

Additionally, the contact pressure played a key role, as it is only at a high contact pressure that the nano-titanium dioxide was present in the transferred material (as shown in Figure 26) and under this condition the lowest coefficient was observed.

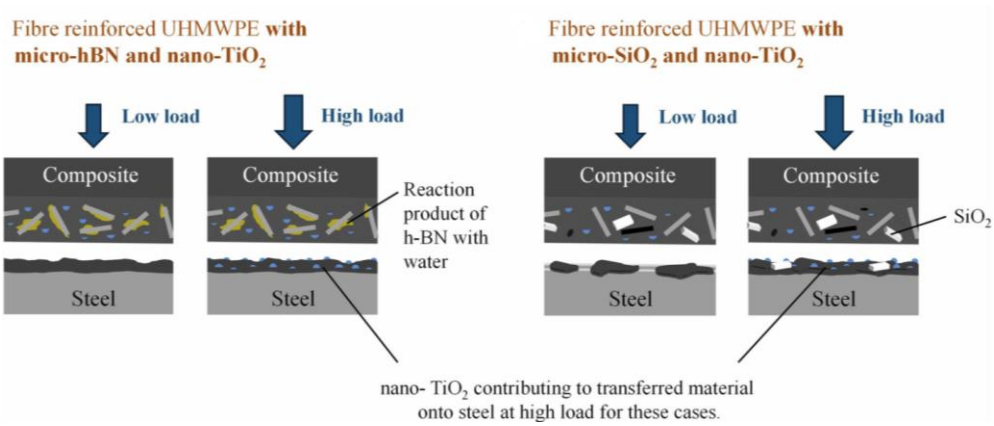

Figure 26 – Illustrations delineating variation in composition of adhered material on steel disc with pressure for compositions containing short carbon fibre, nano- titanium dioxide and micro hexagonal-boron nitride (left) / micro silicon dioxide (right)

With filler–filler interaction now studied in Paper B and Paper C under water lubrication, the next step was to analyse whether the contribution from fillers varies with the lubricant, i.e. to study the filler–lubricant interaction. Additionally, whether the scale effect observed in Paper B persists with a different lubricant. The above forms the basis for the next study, denoted as Paper D.

3.4 Paper D

Title (Tentative)- Role of fillers on the tribological behaviour of UHMWPE composites in environmentially acceptable lubricants.

To understand how the lubricant affects the contribution from different fillers to the tribological performance, various multiscale composites which were noted to perform well under water lubrication were tested with different lubricants. The multiscale composites selected for this study incorporated SCF, graphite, h-BN and titanium dioxide as fillers. Meanwhile, for lubricants, two esters (base and commercial) and a water–glycerol mixture were used as lubricants. The base ester was propylene glycol-based (termed as PG), and the commercial ester used was Panolin Atlantis 5 (termed as Alt in this study). The water–glycerol mixture (termed as WG), on the other hand, was used in a ratio such that its viscosity matched that of the propylene glycol-based ester.

Outcomes from the publication

The tribological tests revealed that the composites had different performance even with lubricants of similar viscosity, implying that the fillers played a critical role in the observed performance.

At 5 MPa, the coefficient of friction with PG ester varied from 0.045 to 0.065 between compositions. Whereas with WG as the lubricant, the mean coefficient of friction was observed to range from 0.009 to 0.023 between compositions, which is 65–79% lower compared to the values with PG ester as lubricant. On the other hand, the mean coefficient of friction observed with Alt as the lubricant was in the 0.03–0.04 range, which was between PG and WG.

At 15 MPa, depending on both the composition and the lubricant, an increase or decrease in the mean coefficient of friction was noted compared to values at 5 MPa. With PG ester as lubricant, the compositions containing graphite exhibited mean coefficient of friction between 0.02 and 0.03 at 15 MPa, whereas in case of graphite-lacking composition, a higher mean coefficient of friction of 0.05 was noted. On other hand with WG as lubricant, the coefficient of friction was again noted to be lower compared to PG for all compositions. The lowest value noted with WG mixture as lubricant was 0.0075, which was for the graphite and h-BN containing nano composition. With Alt ester as lubricant, depending on the composition, an improvement or deterioration in the mean coefficient of friction compared to PG ester was noted at 15 MPa. For compositions containing graphite and h-BN, the coefficient of friction with Alt was 67–82% higher compared to PG ester and was the highest among all compositions with any lubricant. Whereas for compositions containing titanium dioxide, a significantly lower mean coefficient of friction, around 0.018, was noted with Alt as lubricant.

At a low contact pressure of 5 MPa, the specific wear rate with PG ester was noted to be lower compared to the Alt ester and higher compared to the water–glycerol mixture as lubricant, irrespective of the composition. The specific wear rate with PG ester was noted to vary from 4.3E-7 to 6.5E-7 mm^3/Nm between compositions, with the lower value noted for the graphite- and h-BN-containing nano composition, and the highest for the graphite- and titanium dioxide-containing nano composition. With WG as lubricant, the specific wear rate was observed to be the lowest across all compositions compared to other lubricants, with values ranging from 1.8–4.6E-7 mm^3/Nm. Compared to PG as lubricant, WG showed 1.4–2.4 times lower specific wear rate, with higher reductions noted in compositions with h-BN. On the other hand, with Alt ester, the highest wear rate was observed, ranging between 3.9–4.9E-6 mm^3/Nm.

At 15 MPa, depending on both the composition and lubricant, an increase or decrease in the specific wear rate was noted compared to values at 5 MPa. With PG ester as the lubricant, the specific wear rate was noted in range of 7.2-9.3E-7 mm^3/Nm, which is only a marginal variation. In the case of Alt ester, for compositions containing graphite and h-BN, the specific wear rate noted was 4.9–7.9 times higher compared to PG ester, with the value noted for the micro composition, i.e. 5.7E-6 mm^3/Nm, being the highest wear rate among all compositions with any lubricant. Whereas for compositions containing titanium dioxide, a significantly lower specific wear rate of around 5.1E-7 mm^3/Nm was noted with Alt, which is 1.6–1.8 times lower than the specific wear rate observed for the same compositions with PG ester. With WG as lubricant, the compositions containing h-BN were noted to have a lower specific wear rate at 15 MPa in comparison to the other lubricants (2.9–4.4 times lower compared to PG and 2.4–23.4 times lower compared to Alt). The h-BN-lacking composition, on the other hand, showed a specific wear rate of 8.3E-7 mm^3/Nm with the water–glycerol mixture as lubricant, which is similar to the value noted with PG ester. Finally, the lowest specific wear rate at 15 MPa was again noted for the nano composition containing graphite and boron nitride in WG lubricant, which was 1.2–4.1 times lower compared to other compositions in the same lubricant.

The analysis of the worn surfaces provided significant insights into the role of different fillers and possible filler-lubricant interactions in the observed performance:

- The SEM analysis of worn polymer–composite surfaces demonstrated that compositions tested in esters exhibited fibre pullout. In contrast, the compositions tested with the WG mixture did not show this sign. Additionally, optical interferometry conducted on the composite surfaces indicated adhered fibres to have a flatter profile compared to fresh fibres, confirming that fibre thinning occurred in all selected lubricants.

- The SEM analysis of steel disc wear tracks, on the other hand, showed additional material adhered to the steel surfaces lubricated with PG and WG. The AFM analysis

of steel disc wear tracks obtained from testing against graphite-containing compositions with PG and WG as lubricants indicated regions with dimensions similar to the incorporated graphite. Raman analysis of the steel disc wear tracks confirmed the presence of graphite in the material adhered to the steel surface for these compositions.

- The LFM analysis of the material adhered onto the steel surface showed significantly lower lateral force on graphite in steel disc wear tracks lubricated with WG compared to PG.

- In contrast, no additional material was noted on the steel disc wear tracks obtained from testing with Alt, based on SEM and AFM analysis. Additionally, in the wear tracks obtained from testing against titanium dioxide compositions, the roughness of the steel surface was noted to be significantly lower compared to pre-testing, especially along the sliding direction. Moreover, EDS analysis of the worn polymer–composite and steel disc wear tracks indicated the presence of sulphur on surfaces lubricated with Alt.

Conclusion

The selected UHMWPE composites containing various fillers exhibited superior tribological performance with WG as the lubricant compared to an ester of similar viscosity.

With PG ester and WG, carbonaceous fillers (graphite and SCF) contributed directly to tribological performance by participating in transferred material from the polymer composite to the steel surface; boron nitride contributed indirectly and only in the water–glycerol mixture. In contrast, with the commercial Alt ester, material transfer from the polymer composite to the steel disc was significantly hindered; only titanium dioxide exhibited an indirect contribution—and only at elevated contact pressures.

The lubricating property of the graphite transferred onto the steel surface was found to depend on the lubricant, with WG yielding superior performance from the filler compared to the ester. This was because, in the case of WG, the water molecules passivate the defects formed in the carbon lattice during sliding. In contrast, for esters, the long-chain molecules tend to form an adsorbed film, with the polar carbonyl group interacting only weakly with the carbon lattice. Therefore, sliding occurs on the layers of alkyl tails over the graphite surface for esters, resulting in higher lateral force.

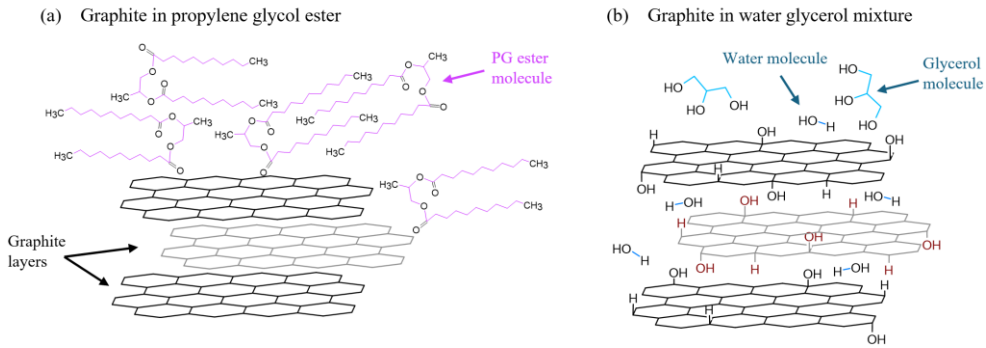

Figure 27 – Schematic illustrating the possible interactions between graphite and the lubricants used in this study. In esters (a), sliding occurs on the layers of alkyl tails over the graphite surface. In contrast, for the water–glycerol mixture (b), sliding takes place on the top carbon lattice layer, with water molecules passivating the defects formed in the graphite structure, thereby facilitating interlayer slip.

Finally, the best performance was noted with the nano composition containing SCF, graphite and h-BN as fillers where the coefficient of friction was noted to be below 0.01 and specific wear rate of around 2E-7 mm^3/Nm. This low friction state was observed to be robust with no effect from changing sliding parameters or start-stop conditions as shown in Figure 28.

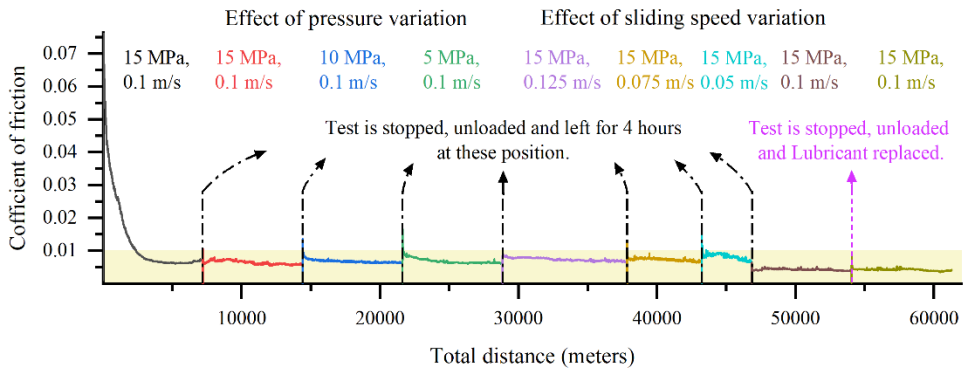

Figure 28 – Variation in coefficient of friction obtained from reciprocating tests conducted in pin-on-disc arrangement with $Gr_M + BN_{M+N}$ and 316L steel as surfaces and water-glycerol mixture (WG) as the lubricant. The sliding conditions were varied every 20 hours into the test, with conditions shown above.

CHAPTER 4

Conclusion and Future aspects

Upon a comprehensive review of the existing literature, various key gaps and issues were identified across the available foundational work in the field. These issues directly contributed to the formulation of the research hypotheses and goals that guide this thesis.

Prior to jumping into the hypothesis, the work began with tackling the known issues with the polymer materials and fillers of interest. This was done by using additives during manufacturing. The above step was necessary to have composites that are viable for use in real world applications. Upon doing work and finding the solutions that worked to resolve the known issues a decisive choice needed to be made, i.e. to use additive and reducing the filler concentration or finding another solution to known issues. After careful reasoning the later was selected.

Thereby various UHMWPE composites were manufactured containing different fillers to study the hypothesis. These composites had various carbonaceous and non-carbonaceous fillers and of different scale. The testing of these composites has contributed to the scientific knowledge in the following ways

- More scientific studies now exist relating to which filler combinations perform better, with this research providing clear evidence on which material pairs—particularly the difference between carbonaceous–carbonaceous and carbonaceous–non-carbonaceous filler pairs—affects composite properties and tribological performance.

- A better understanding has been developed on whether composite properties and tribological performance observed in multi-scale composites arise from filler scale, material type, or both, as this work systematically decouples these parameters to examine their individual and combined effects.

- More clarity now exists regarding filler–filler interactions, with this study showing how different filler types may influence one another's performance and contribute either synergistically or antagonistically to the overall behaviour of the composite.

- The influence of lubricants on filler performance is now better understood, as this research helps separate the effects of viscosity from those of filler–lubricant interactions, shedding light on their distinct roles in enhancing or diminishing tribological outcomes.

Ultra-high-molecular-weight polyethylene composites incorporating various fillers (short carbon fibres, graphite, boron nitride, silicon dioxide and titanium dioxide) were prepared. From the observed variation in composite properties, the following conclusions can be drawn:

- The incorporation of multiple fillers in the composite material led to enhancement of selective composite properties, for example hardness, as incorporation of several fillers showed greater hardness values than have single filler. Furthermore, the filler scale was found to influence hardness, as having nano-scale fillers yielded higher hardness than micro-scale filler in same concentration.

- Selective composite properties were also noted to depend on filler type and not scale, such as crystallinity of the polymer material. Upon having only carbonaceous fillers in the polymer-composite a reduction in crystallinity was observed, which declined steadily upon having more carbonaceous fillers. However, when non-carbonaceous fillers were introduced into the composition, the reduction in crystallinity abated.

- Surface wettability of the manufactured composites also implied filler type to play key role rather than the scale. Further when more than one filler was present the overall nature of the surface was the sum of the individual effects. However, in all cases the composites remained on the hydrophobic side based on contact angel measurements.

Upon testing these manufactured Ultra-high-molecular-weight polyethylene composites against 316L stainless steel under water lubricated condition, the following conclusions could be drawn:

- It was confirmed that incorporation of several fillers into the polymer led to improvement in tribological performance from the resulting composite against steel under water lubricated condition.

- Additionally, it was noted that both the filler type and scale played a role in the observed improvement, as incorporating nano-scale filler provided better performance than having their micro-scale equivalents in same concentration.

- When several fillers are incorporated, it was noted that the presence of one filler could alter the contribution from another filler, thereby confirming filler-filler interaction. For instance, with hexagonal-boron nitride present as filler, the short carbon fibres remained adhered, which would otherwise have been easily pulled out in the absence of hexagonal-boron nitride.

- Not all filler-filler interaction were noted to provide a positive outcome. For example, having graphite as filler hindered the transfer of other fillers to from the

composite to steel surface, altering the composition of the beneficial transfer film and thereby the observed tribological performance.

Lastly, upon testing these manufactured Ultra-high-molecular-weight polyethylene composites against 316L stainless steel under alternate lubricants such as esters and water-glycerol mixtures, the following conclusions could be drawn:

- The selected composites exhibited diverse effects in different lubricants, showing lower coefficient of friction and wear rates in water-glycerol mixture compared with ester of same viscosity.

- The contribution from fillers varied with lubricant, thereby confirming the filler-lubricant interaction happening alongside to the filler-filler interaction. For example, graphite was noted to provide better lubricating property in water-glycerol mixture than in esters.

- Additionally, the effect of filler scale on the tribological performance initially noted with water lubrication was noted to persist, but only with water-glycerol mixture. Where again, the composition containing nano-scale filler performed better compared to micro-scale filler containing composition for the same concentration of fillers.

It was noted that when interactions between components are favourable, effect of filler scale is utilized, and with selective fillers incorporated into the composition a state of superlubricity can be achieved in polymer composite-steel contacts. This state is robust and can be attained for prolonged sliding durations. Moreover, it does not require any unpractical conditions such as ultra smooth surfaces, specific atmospheric conditions or toxic materials.

While this work aims to provide comprehensive knowledge on the individual roles of filler material and scale, the nature and effect of filler–filler and filler–lubricant interactions to overall performance; numerous new openings appeared while the course of this study that offer scope for future work

- Based on the results noted in this work, aqueous glycerol mixtures show great potential to be use with polymer-composites. This requires other polyhydric alcohols to also be explored for their lubricating potential in polymer composite-steel contacts.

- Upon testing commercial ester with multi-scale composites, it was observed that the transfer of material from the composite to steel surface was greatly impeded, possibly from the additives present in the lubricant. This requires exploration on which additives are favourable for use in polymer composite-steel contacts.

- As the transportation sector shifts towards electrification, it is essential to examine how the contribution from fillers and other observed effects evolve under applied electric fields.

References

1. K. Holmberg and A. Erdemir, “Influence of tribology on global energy consumption, costs and emissions,” Friction, vol. 5, no. 3, pp. 263–284, 2017.
2. CHAPTER 7: Resistance and Powering of Ships. Public source. Link: https://www.usna.edu/NAOE/_files/documents/Courses/EN400/02.07_Chapter_7.pdf
3. European Commission, “2023 Report from the European Commission on CO_2 Emissions from Maritime Transport (COM(2024) 151 final),” Brussels, Apr. 8, 2024
4. Statista, “Transport CO_2 emissions shares by type,” Accessed Aug. 11, 2025. [Online]. Available: https://www.statista.com/statistics/1185535/transport-carbon-dioxide-emissions-breakdown/
5. Statista, “Global shipping CO_2 emissions 1970–2023,” Accessed Aug. 11, 2025. [Online]. Available: https://www.statista.com/statistics/1291468/international-shipping-emissions-worldwide/
6. E. Quaranta and P. Davies, “Emerging and innovative materials for hydropower engineering applications: Turbines, bearings, sealing, dams and waterways, and ocean power,” Engineering, vol. 8, pp. 148–158, 2022.
7. Y. Ji, H. Song, Z. Xue, Z. Li, M. Tong, and H. Li, “A review of the efficiency improvement of hydraulic turbines in energy recovery,” Processes, vol. 11, no. 6, p. 1815, 2023.
8. R. Zhu, X. Zhang, Q. Huang, S. Li, and Q. Fu, “Predicting the remaining life of centrifugal pump bearings using the KPCA–LSTM algorithm,” Energies, vol. 17, 2024.
9. M. Irfan, M. A. Hanif, M. Z. Khalid, K. Latif, S. A. Khan, and H. Ali, “Condition monitoring of water pump bearings using ensemble classifier,” Advances in Mechanical Engineering, vol. 14, 16878132221089170, 2022.
10. Ship Technology, “Poll: Is the shipping industry doing enough to curb carbon emissions?,” Accessed Aug. 11, 2025. [Online]. Available: https://www.ship-technology.com/features/shipping-carbon-emissions/
11. Western Machine Works, “Hydro turbine thrust bearing,” Accessed Aug. 11, 2025. [Online]. Available: https://westernmachine.com/hydro-turbine-thrust-bearing/
12. A. Majidov, “Understanding bearing failures in centrifugal pumps: Causes and prevention,” LinkedIn, Accessed Aug. 11, 2025. [Online]. Available: https://www.linkedin.com/pulse/understanding-bearing-failures-centrifugal-pumps-causes-aydin-majidov-jjklf/
13. W. Wang and J. Qu, “Current and candidate additives for environmentally acceptable lubricants—A review,” Friction, advance online publication, 2024.
14. A. Z. Syahir, M. A. Zaki, M. Syazwan, N. A. Syahrullail, M. I. Zulkifli, and N. A. Masjuki, “A review on bio-based lubricants and their applications,” Journal of Cleaner Production, vol. 168, pp. 997–1016, 2017.
15. U.S. Environmental Protection Agency, Office of Wastewater Management, Environmentally acceptable lubricants. Washington, DC: U.S. EPA, 2011.
16. X. Dai, J. Lv, P. Fu, and S. Guo, “Microbial remediation of oil-contaminated shorelines: A review,” Environmental Science and Pollution Research, vol. 30, pp. 93491–93518, 2023.
17. R. Shankar, J. Kaur, S. K. Mehta, and S. Basu, “Environmental significance of lubricant oil: A systematic study of photooxidation and its consequences,” Water Research, vol. 168, 115140, 2020.
18. M. I. Matilda and H. S. Samuel, “Bioremediation of oil spill: Concept, methods and applications,” Discover Chemical Engineering, vol. 1, p. 42, 2024.
19. X. Dai, J. Lv, P. Fu, and S. Guo, “Microbial remediation of oil-contaminated shorelines: A review,” Environmental Science and Pollution Research, vol. 30, pp. 93491–93518, 2023.
20. J. Pargeter, “Oil spill threatens a treasured coral atoll in the South Pacific,” The New York Times, Mar. 6, 2019. Accessed Aug. 11, 2025. [Online]. Available: https://www.nytimes.com/2019/03/06/world/australia/solomon-islands-oil-spill-unesco.html
21. NDTV, “Another Manipur River Contaminated With Oil-Like Substance, Dam Gates Shut,” Feb. 8, 2024. Accessed Aug. 11, 2025. [Online]. Available: https://www.ndtv.com/india-news/another-manipur-river-iril-turel-contaminated-with-oil-like-substance-dolaithabi-dam-gates-shut-5014569

22. M. Miller, “Additives for bioderived and biodegradable lubricants,” in Lubricant Additive Chemistry and Applications, 2nd ed., L. R. Rudnick, Ed. Boca Raton, FL, USA: CRC Press, 2017, pp. 421–429.
23. R. Shah, M. Woydt, and S. Zhang, “The economic and environmental significance of sustainable lubricants,” Lubricants, vol. 9, no. 2, p. 21, 2021.
24. D. Gnanasekaran and V. P. Chavidi, “Biodegradable, renewable, and eco-friendly vegetable oil: Lubricants,” in Vegetable Oil Based Bio-Lubricants and Transformer Fluids: Applications in Power Plants, Singapore: Springer, 2018, pp. 29–47.
25. A. M. Tamothran, K. Bhubalan, S. T. Anuar, and J. M. Curtis, “The degradation and toxicity of commercially traded vegetable oils following spills in aquatic environment,” Environmental Research, vol. 214, pt. 3, 113985, 2022.
26. W. V. Smith, “Material selection criteria for water lubrication,” Wear, vol. 25, no. 2, pp. 139–153, 1973.
27. R. Pai and D. J. Hargreaves, “Water lubricated bearings in Green Tribology: Biomimetics, Energy Conservation and Sustainability”, M. Nosonovsky and B. Bhushan, Eds. Berlin, Heidelberg: Springer, 2012, pp. 347–391.
28. J. Kogovšek and M. Kalin, “Lubrication performance of graphene-containing oil on steel and DLC-coated surfaces,” Tribology International, vol. 138, pp. 59–67, 2019.
29. Royal Society of Chemistry, Glycerol: Properties and Production. Cambridge, UK: RSC, 2008, pp. 1–17.
30. C. Chen, W. Z. Li, Y. C. Song, and J. Yang, “Hydrogen bonding analysis of glycerol aqueous solutions: A molecular dynamics simulation study,” Journal of Molecular Liquids, vol. 146, pp. 23–28, 2009.
31. V. F. Naeini, M. Björling, J. A. Larsson, and R. Larsson, “Tribochemistry of glycerol–water mixtures confined between ferrous substrates: An atomic-scale concept by reactive molecular dynamics simulation,” Tribology International, 2025.
32. A. V. Egorov, A. P. Lyubartsev, and A. Laaksonen, “Molecular dynamics simulation study of glycerol–water liquid mixtures,” The Journal of Physical Chemistry B, vol. 115, pp. 14572–14581, 2011.
33. J. L. Dashnau, N. V. Nucci, K. A. Sharp, and J. M. Vanderkooi, “Hydrogen bonding and the cryoprotective properties of glycerol/water mixtures,” The Journal of Physical Chemistry B, vol. 110, pp. 13670–13677, 2006.
34. P. Okhiria, M. Björling, P. Johansson, M. Hasan, R. Larsson, & Y. Shi, “Tribological performance of glycerol-based hydraulic fluid under low-temperature conditions,” Lubricants, vol. 12 (12), 430, 2024.
35. J. G. Z. Tamayo, M. Björling, Y. Shi, B. Prakash, and R. Larsson, “Micropitting performance of glycerol-based lubricants under rolling-sliding contact conditions,” Tribology International, vol. 167, 107348, 2022.
36. J. Bosch and C. DellaCorte, “Rheological characterization and tribological evaluation of water-based lubricants in AISI 52100 bearing steel,” Tribology Letters, vol. 72, no. 1, p. 10, 2023.
37. V. Sivabalan, B. Walid, Y Madec, A. Qasim, B. Lal, “Corrosion inhibition study on glycerol as simultaneous gas hydrate and corrosion inhibitor in gas pipelines,” Malaysian Journal of Analytical Sciences, vol. 24, 2024.
38. Zubaidi, I. A., Jones, R., Alzughaibi, M., Albayyadhi, M., Darzi, F., & Ibrahim, H, “Crude glycerol as an innovative corrosion inhibitor,” Applied System Innovation, 2018.
39. M. D. de Jesus Almeida, C. A. Della Rovere, L. R. P. de Andrade Lima, D. V. Ribeiro, and C. A. C. De Souza, “Glycerol effect on the corrosion resistance and electrodeposition conditions in a zinc electroplating process,” Materials Research, vol. 22, e20180480, 2019.
40. M. H. Moklis, S. Cheng, and J. S. Cross, “Current and future trends for crude glycerol upgrading to high value-added products,” Sustainability, vol. 15, no. 14, 11604, 2023.
41. M. Padhan, U. Marathe, and J. Bijwe, “Tribology of poly(ether ketone) composites based on nanoparticles of solid lubricants,” Composites Part B: Engineering, vol. 201, 108323, 2020.
42. Polymers Australia, “Polymers | Thermoplastics,” Accessed Aug. 11, 2025. [Online]. Available: https://polymers.com.au/thermoplastics/#
43. G. Wypych, Handbook of Polymers, 2nd ed. Amsterdam, Netherlands: Elsevier, 2016.
44. Knowde, “G-PAEK 1200G — Gharda Chemicals — Knowde,” Accessed Aug. 11, 2025. [Online]. Available: https://www.knowde.com/stores/gharda-chemicals/products/g-paek-1200g
45. A. Golchin, G. F. Simmons, S. Glavatskih, and B. Prakash, “Tribological behaviour of polymeric materials in water-lubricated contacts,” Proceedings of the Institution of Mechanical Engineers, Part J: Journal of Engineering Tribology, vol. 227, no. 8, pp. 811–825, 2013.

46. A. Golchin, K. Friedrich, A. Noll, and B. Prakash, "Tribological behavior of carbon-filled PPS composites in water lubricated contacts," Wear, vols. 328–329, pp. 456–463, 2015.
47. J. Chen, J. Jia, H. Zhou, J. Chen, S. Yang, L. Fan, "Tribological behavior of short-fiber-reinforced polyimide composites under dry-sliding and water-lubricated conditions," Journal of Applied Polymer Science, 2008.
48. C. Min, P. Nie, H.-J. Song, Z. Zhang, and K. Zhao, "Study of tribological properties of polyimide/graphene oxide nanocomposite films under seawater-lubricated condition," Tribology International, vol. 80, pp. 131–140, 2014.
49. K. Tanaka, "Friction and wear of semicrystalline polymers sliding against steel under water lubrication," Journal of Tribology, vol. 102, no. 4, pp. 526–533, 1980.
50. D. C. Evans, "Polymer–fluid interaction in relation to wear," in Wear Control of Materials, London, U.K.: Mechanical Engineering Publications Ltd., 1987, pp. 47–55.
51. Y. Yamamoto and T. Takashima, "Friction and wear of water lubricated PEEK and PPS sliding contacts," Wear, vol. 253, no. 7–8, pp. 820–826, 2002.
52. X. Hu, "Friction and wear behaviors of toughened polyoxymethylene blend under water lubrication," Polymer-Plastics Technology and Engineering, vol. 39, no. 1, pp. 137–150, 2000.
53. J. Wang, F. Yan, and Q. Xue, "Tribological behavior of PTFE sliding against steel in sea water," Wear, vol. 267, nos. 9–10, pp. 1634–1641, 2009.
54. D. Xiong and S. Ge, "Friction and wear properties of UHMWPE/Al_2O_3 ceramic under different lubricating conditions," Wear, vols. 250–251, pp. 242–245, 2001.
55. O. Jacobs, R. Jaskulka, F. Yang, and W. Wu, "Sliding wear of epoxy compounds against different counterparts under dry and aqueous conditions," Wear, vol. 256, nos. 1–2, pp. 9–15, 2004.
56. J. Bijwe, S. Sharma, M. Sharma, T. Parida, and P. Trivedi, "Exploration of potential of solid lubricants and short fibers in Polyetherketone (PEK) composites," Wear, vol. 301, nos. 1–2, pp. 810–819, 2013.
57. J. N. Panda, J. Bijwe, and R. K. Pandey, "Optimization of the amount of short glass fibers for superior wear performance of PAEK composites," Composites Part A: Applied Science and Manufacturing, vol. 116, pp. 158–168, 2019.
58. Y. Yamamoto and M. Hashimoto, "Friction and wear of water lubricated PEEK and PPS sliding contacts. Part 2. Composites with carbon or glass fibre," Wear, vol. 257, nos. 1–2, pp. 181–189, 2004.
59. H.-J. Song, N. Li, J. Yang, C.-Y. Min, and Z.-Z. Zhang, "Preparation and tribological behaviors of poly(ether ether ketone) nanocomposite films containing graphene oxide nanosheets," Journal of Nanoparticle Research, vol. 15, 2013.
60. Z. Yang, Z. Guo, and C. Yuan, "Effects of MoS_2 microencapsulation on the tribological properties of a composite material in a water-lubricated condition," Wear, vols. 432–433, 102919, 2019.
61. K. S. Randhawa and A. Patel, "The effect of environmental humidity/water absorption on tribo-mechanical performance of polymers and polymer composites – a review," Industrial Lubrication and Tribology, 2021.
62. American Elements, "Carbon Fiber," Accessed July, 2025. [Online]. Available: https://www.americanelements.com/carbon-fiber-7440-44-0
63. GLT Products, "Properties of Glass Fiber," Accessed July, 2025. [Online]. Available: https://blog.gltproducts.com/blog/glass-fiber-properties
64. A. Kelly, Concise Encyclopedia of Composite Materials. Amsterdam, Netherlands: Elsevier, 2012.
65. J. N. Panda, Design and Development of High-Performance Polymer Composites and Self-Lubricating Bearings, Ph.D. thesis, Indian Institute of Technology Delhi, 2019.
66. H. Zeng, G. He, and G. Yang, "Friction and wear of poly(phenylene sulphide) and its carbon fibre composites: I unlubricated," Wear, vol. 116, pp. 59–68, 1987.
67. B. K. Yen, "Influence of water vapor and oxygen on the tribology of carbon materials with sp2 valence configuration," Wear, 1996.
68. C.P. Gao, G.F. Guo, F.Y. Zhao, T.M. Wang, B. Jim, B. Wetzel, G. Zhang, Q.H. Wang "Tribological behaviors of epoxy composites under water lubrication conditions," Tribology International, vol. 95, pp. 333–341, 2016.
69. R. K. Iler, The Chemistry of Silica: Solubility, Polymerization, Colloid and Surface Properties, and Biochemistry. New York, NY, USA: Wiley, 1979.
70. T. Sugita, K. Ueda, and Y. Kanemura, "Material removal mechanism of silicon nitride during rubbing in water," Wear, 1984.
71. T. E. Fischer and H. Tomizawa, "Interaction of tribochemistry and microfracture in the friction and wear of silicon nitride," Wear, 1985.

72. J. Shi, R. Yao, Z. Kong, F. Ni, and J. Zheng, “Strength analysis on hybrid welding interface of polymer and short carbon fiber reinforced composite,” Journal of Materials Science, vol. 56, pp. 14556–14569, 2021.
73. Graft Polymer d.o.o., “GRAFTABOND Products TDS & MSDS,” Accessed July, 2025. [Online]. Available: https://graftpolymer.com/download/graftabond/
74. N. G. Karsli and A. Aytac, “Effects of maleated polypropylene on the morphology, thermal and mechanical properties of short carbon fiber reinforced polypropylene composites,” Materials & Design, vol. 32, pp. 4069–4073, 2011.
75. F. Lv, Y. Wang, Y. Song, Y. Yang, J. Wang, Y. Cao, C. Li, W. Wang, “A facile rheological approach for the determination of ‘super toughness point’ of nylon1212/POE-g-MAH/MWCNT nanocomposites,” Composites Science and Technology, vol. 177, pp. 73–80, 2019.
76. I. Nadeem, M. Malok, J. Kovač, T. B. Yaqub, A. Cavaleiro, “Superior macro-scale tribological performance of steel contacts based on graphene quantum dots in aqueous glycerol,” Tribology International, vol. 181, 108328, 2023.
77. S. Bhowmick, A. Banerji, and A. T. Alpas, “Role of humidity in reducing sliding friction of multilayered graphene,” Carbon, vol. 87, pp. 374–384, 2015.
78. B. K. Yen, B. E. Schwickert, and M. F. Toney, “Origin of low-friction behavior in graphite investigated by surface X-ray diffraction,” Applied Physics Letters, vol. 84, pp. 4702–4704, 2004.
79. East Carbon, “Graphite Structure Explained: From Layers, Molecular Forces to Anisotropy,” Accessed July, 2025. [Online]. Available: https://www.eastcarb.com/graphite-structure/
80. Y. A. Golubev and I. V. Antonets, “Electrophysical properties and structure of natural disordered sp2 carbon,” Nanomaterials, vol. 12, 2022.
81. J. H. Jia, J. M. Chen, H. D. Zhou, J. B. Wang, and H. Zhou, “Friction and wear properties of bronze–graphite composite under water lubrication,” Tribology International, vol. 37, no. 5, pp. 423–429, 2004.
82. G. Cui, Q. Bi, S. Zhu, J. Yang, and W. Liu, “Tribological properties of bronze–graphite composites under sea water condition,” Tribology International, vol. 53, pp. 76–86, 2012.
83. H. A. Al-Turaif, “Effect of nano TiO_2 particle size on mechanical properties of cured epoxy resin,” Progress in Organic Coatings, vol. 69, pp. 241–246, 2010.
84. M. C. Kuo, C. M. Tsai, J. C. Huang, and M. Chen, “PEEK composites reinforced by nano-sized SiO_2 and Al_2O_3 particulates,” Materials Chemistry and Physics, vol. 90, pp. 185–195, 2005.
85. G. Zhang, A. K. Schlarb, S. Tria, and O. Elkedim, “Tensile and tribological behaviors of PEEK/nano-SiO_2 composites compounded using a ball milling technique,” Composites Science and Technology, vol. 68, pp. 3073–3080, 2008.
86. N. Liu, J. Wang, J. Yang, G. Han, and F. Yan, “Combined effect of nano-SiO_2 and nano-Al_2O_3 on improving the tribological properties of Kevlar fabric/phenolic laminate in water,” Tribology Transactions, vol. 59, pp. 163–169, 2016.
87. Q. H. Wang, Q. J. Xue, W. M. Liu, and J. M. Chen, “Effect of nanometer SiC filler on the tribological behavior of PEEK under distilled water lubrication,” Journal of Applied Polymer Science, vol. 78, no. 3, pp. 609–616, 2000.
88. Q. H. Wang, Q. J. Xue, W. M. Liu, and J. M. Chen, “Tribological characteristics of nanometer Si3N4 filled poly(ether ether ketone) under distilled water lubrication,” Journal of Applied Polymer Science, vol. 79, no. 8, pp. 1394–1400, 2001.
89. X. Li, Y. Gao, Q. Yang, W. Pan, Y. Li, Z. Zhong, L. Song, “Evaluation of tribological behavior of B4C–hBN ceramic composites under water-lubricated condition,” Ceramics International, vol. 41, pp. 7387–7393, 2015.
90. X. Li, Y. Gao, and Q. Yang, “Sliding tribological performance of B4C–hBN composite ceramics against AISI 321 steel under distilled water condition,” Ceramics International, vol. 43, pp. 14932–14937, 2017.
91. W. Chen, Z. Wang, X. Liu, J. Jia, and Y. Hua, “Effect of load on the friction and wear characteristics of Si3N4–hBN ceramic composites sliding against PEEK in artificial seawater,” Tribology International, vol. 141, 105902, 2020.
92. C. Gao, G. Guo, G. Zhang, Q. Wang, T. Wang, H. Wang, “Formation mechanisms and functionality of boundary films derived from water lubricated polyoxymethylene/hexagonal boron nitride nanocomposites,” Materials & Design, vol. 115, pp. 276–286, 2017.
93. A. Kurdi, H. Wang, and L. Chang, “Effect of nano-sized TiO_2 addition on tribological behaviour of poly ether ether ketone composite,” Tribology International, vol. 117, pp. 225–235, 2018.

94. H J Song, Z Z Zhang, X H Men, "The tribological behaviors of the polyurethane coating filled with nano-SiO_2 under different lubrication conditions," Composites Part A: Applied Science and Manufacturing, vol. 39, pp. 188–194, 2008.
95. American Chemical Society, "Boron nitride — Molecule of the Week," Accessed July, 2025. [Online]. Available: https://www.acs.org/molecule-of-the-week/archive/b/boron-nitride.html
96. Sukhmani Impex, "Unveiling the distinctions: Rutile vs Anatase Titanium dioxide (TiO_2)," Accessed July, 2025. [Online]. Available: https://sukhmaniimpex.com/unveiling-the-distinctions-rutile-vs-anatase-titanium-dioxide-tio2/
97. King's College London, "Surface modification of titanium and titanium alloys to enhance bone healing," Thesis page, Accessed July, 2025. [Online]. Available: https://kclpure.kcl.ac.uk/portal/en/studentTheses/surface-modification-of-titanium-and-titanium-alloys-to-enhance-b
98. A. Kurdi, H. Wang, and L. Chang, "Effect of nano-sized TiO2 addition on tribological behaviour of poly ether ether ketone composite," Tribology International, vol. 117, pp. 225–235, 2018.
99. S. Li, C. Dong, C. Yuan, and X. Bai, "Effects of TiO2 nano-particles on wear-resistance and vibration-reduction properties of a polymer for water-lubricated bearing," Wear, vol. 522, 204713, 2023.
100. V G Nguyen, H Thai, D H Mai, H T Tran, D L Tran, M T Vu, "Effect of titanium dioxide on the properties of polyethylene/TiO2 nanocomposites," Composites Part B: Engineering, vol. 45, pp. 1192–1198, 2013.
101. M. Padhan, A. Gulhane, and J. Bijwe, "Composites of titanium nano and micro-particles and UHMWPE for enhanced performance properties," Surface Topography: Metrology and Properties, vol. 8, 025013, 2020.
102. M. Padhan, G. Paul, and J. Bijwe, "Roles of size, shape, amount, and functionalization of nanoparticles of titania in controlling the tribo-performance of UHMWPE composites," Frontiers in Materials, vol. 7, 2020
103. K. Kumar, Investigations on possible synergism of two solid lubricants of varying sizes and amounts in polymer composites, Thesis, Indian Institute of Technology Delhi, 2014.
104. L. Chang, Z. Zhang, L. Ye, and K. Friedrich, "Synergistic effects of nanoparticles and traditional tribofillers on sliding wear of polymeric hybrid composites," in Tribology of Polymeric Nanocomposites, 2nd ed., Elsevier, 2013, pp. 49–89.
105. C.-P. Gao, S.-Q. Fan, S.-S. Zhang, P. Zhang, and Q.-H. Wang, "Enhancement of tribofilm formation from water lubricated PEEK composites by copper nanowires," Applied Surface Science, vol. 444, pp. 364–376, 2018.
106. H. S. Vadivel, A. Golchin, and N. Emami, "Tribological behaviour of carbon filled hybrid UHMWPE composites in water," Tribology International, vol. 124, pp. 169–177, 2018.
107. B. Chen, J. Wang, N. Liu, and F. Yan, "Synergism of several carbon series additions on the microstructures and tribological behaviors of polyimide-based composites under sea water lubrication," Materials & Design, vol. 63, pp. 325–332, 2014.
108. Sigma-Aldrich, "Polyethylene-graft-maleic anhydride 500 cP 140°C 9006-26-2," Product page, Accessed July, 2025. [Online]. Available: https://www.sigmaaldrich.com/SI/en/product/aldrich/456624
109. Aksit, M., Gröschel, S., Kuhn, U., Aksit, A., Kreger, K., Schmidt, H.-W., & Altstädt, V. "Low-density polybutylene terephthalate foams with enhanced compressive strength via a reactive-extrusion process," Polymers, vol. 12, no. 11, 2682, 2020.
110. B. Chen, J. Wang, and F. Yan, "Friction and wear behaviors of several polymers sliding against GCr15 and 316 steel under the lubrication of sea water," Tribology Letters, vol. 42, pp. 17–25, 2011.
111. Y. Xu, H. Qi, G. Li, X. Guo, Y. Wan, G. Zhang, "Significance of an in-situ generated boundary film on tribocorrosion behavior of polymer–metal sliding pair," Journal of Colloid and Interface Science, vol. 518, pp. 263–276, 2018.
112. J. Wang, F. Yan, and Q. Xue, "Tribological behavior of PTFE sliding against steel in sea water," Wear, vol. 267, nos. 9–10, pp. 1634–1641, 2009.
113. B. Chen, J. Wang, and F. Yan, "Microstructure of PTFE-based polymer blends and their tribological behaviors under aqueous environment," Tribology Letters, vol. 45, pp. 123–132, 2012.
114. P. Martins Ferreira, B. Trindade, and M. Kalin, "Aging of polyetheretherketone (PEEK) and polyphthalamide (PPA) in polar and non-polar lubricant base oils," Polymer Testing, vol. 131, 108342, 2024.

115. A. Golchin, A. Wikner, and N. Emami, “An investigation into tribological behaviour of multi-walled carbon nanotube/graphene oxide reinforced UHMWPE in water lubricated contacts,” Tribology International, vol. 95, pp. 156–161, 2016.
116. A. Golchin, A. Villain, and N. Emami, “Tribological behaviour of nanodiamond reinforced UHMWPE in water-lubricated contacts,” Tribology International, vol. 110, pp. 195–200, 2017.
117. M. Hedenqvist and U. W. Gedde, “Diffusion of small-molecule penetrants in semicrystalline polymers,” Progress in Polymer Science, vol. 21, no. 2, pp. 299–333, 1996.
118. J. Wang, B. Chen, N. Liu, G. Han, and F. Yan, “Combined effects of fiber/matrix interface and water absorption on the tribological behaviors of water-lubricated polytetrafluoroethylene-based composites reinforced with carbon and basalt fibers,” Composites Part A: Applied Science and Manufacturing, vol. 59, pp. 85–92, 2014.

Department of Engineering Sciences and Mathematic
Division of Machine Elements

ISSN 1402-1544
ISBN 978-91-8048-933-1 (print)
ISBN 978-91-8048-934-8 (pdf)

Luleå University of Technology 2025

LULEÅ
UNIVERSITY
OF TECHNOLOGY